Electronic Supplementary Material (ESI) for ChemComm.

Multicolor Protein FRET with Tryptophan, Selective Coumarin-Cysteine Labeling, and Genetic Acridonylalanine Encoding

John J. Ferrie,[a,‡] Naoya Ieda,[a,b,‡] Conor M. Haney,[a] Christopher R. Walters,[a] Itthipol Sungwienwong,[a] Jimin Yoon,[a] and E. James Petersson[a,*]

a. Department of Chemistry, University of Pennsylvania, 213 South 34th Street, Philadelphia, PA 19104, USA.

b. Current address: Department of Organic and Medicinal Chemistry, Graduate School of Pharmaceutical Sciences, Nagoya City University, 3-1, Tanabedori, Mizuho-ku, Nagoya-shi, Aichi 467-8603, Japan

[‡] *These authors contributed equally to this work.*

Table of Contents

General Information

Materials. *E. coli* BL21(DE3) cells were purchased from Stratagene (La Jolla, CA, USA). Milli-Q filtered (18 MΩ) water was used for all solutions (Millipore; Billerica, MA, USA). Bradford reagent assay kits were purchased from BioRAD (Hercules, CA, USA). Amicon Ultra centrifugal filter units (3 kDa MWCO) were purchased from EMD Millipore. All other reagents and solvents were purchased from Fisher Scientific (Pittsburgh, PA, USA) or Sigma-Aldrich unless otherwise specified. DNA sequencing was performed at the University of Pennsylvania DNA sequencing facility.

Instruments. Low resolution electrospray ionization mass spectra (LRMS) were obtained on a Waters Acquity Ultra Performance LC connected to a single quadrupole detector (SQD) mass spectrometer (Milford, MA, USA). High resolution electrospray ionization mass spectra (HRMS) were collected with a Waters LCT Premier XE liquid chromatograph/mass spectrometer. Nuclear magnetic resonance (NMR) spectra were obtained on a Bruker DRX 500 MHz instrument (Billerica, MA, USA). Matrix assisted laser desorption/ionization with time-of-flight detector (MALDI-TOF) mass spectra were acquired on a Bruker Ultraflex III instrument. UV-Vis absorption spectra were acquired on a Hewlett-Packard 8452A diode array spectrophotometer (currently Agilent Technologies; Santa Clara, CA, USA). Fluorescence spectra were collected with a Tecan M1000 plate reader (Mannedorf, Switzerland) or on a Photon Technologies International (PTI) QuantaMaster40 fluorometer (currently Horiba Scientific, Edison, NJ, USA). Time-dependent fluorescence readings were made on a Tecan M1000 plate reader.

Chemical Synthesis

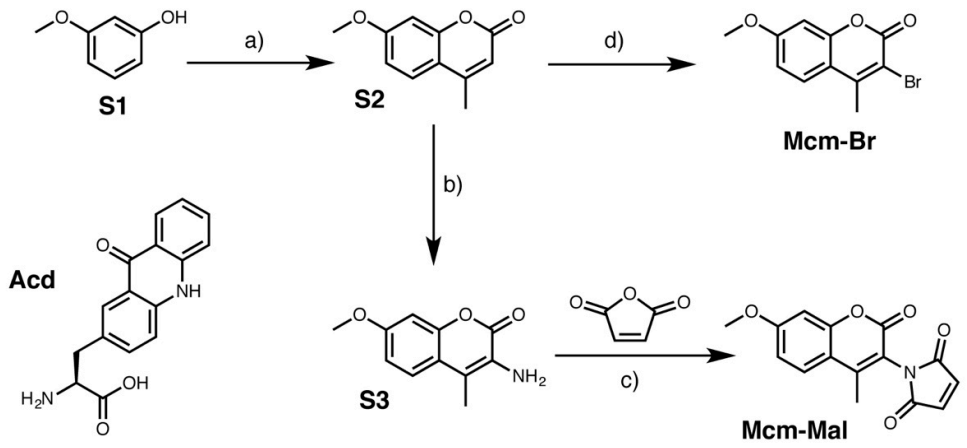

Scheme S1. Synthesis of Mcm-Br and Mcm-Mal. a) Ethyl acetoacetate, H_2SO_4, 65%; b) 1. Ac_2O, HNO_3; 2) H_2 (g), Pd/C, 32% (over two steps); c) Maleic anhydride, 84%; d) NBS, NH_4OAc, 78%

7-methoxy-4-methyl-2*H*-chromen-2-one (**S2**). 3-Methoxyphenol (**S1**, 988 μL, 9.00 mmol) and ethyl acetoacetate (1722 μL, 13.50 mmol, 1.5 equiv.) were dissolved into conc. H_2SO_4 (10 mL) slowly. The reaction mixture was stirred at room temperature (RT) for 3 hours. The reaction mixture was poured into water (50 mL) on ice water bath and stirred for 1 hour. The precipitate was collected on Buchner funnel. The white solid was dissolved into CH_2Cl_2. This solution was washed with brine and dried over Na_2SO_4. Filtration, evaporation, and purification by silica gel flash chromatography (*n*-hexane/EtOAc = 2/1 → 1/1 → EtOAc only) gave 1112 mg (65%) as white solid: ^{1}H NMR ($CDCl_3$, 500 MHz, δ; ppm) 7.50 (1H, d, J = 8.5 Hz), 6.87 (1H, dd, J = 2.5 Hz, 8.5 Hz), 6.83 (1H, d, J = 2.5 Hz), 6.14 (1H, s), 3.88 (3H, s), 2.41 (3H, s); ^{13}C NMR ($CDCl_3$, 125 MHz, δ; ppm) 162.9, 161.5, 155.6, 152.7, 125.7, 113.8, 112.5, 112.2, 101.1, 56.0, 18.9; R_f value 0.79 (*n*-hexane/ EtOAc = 3/2); HRMS (ESI) Calcd. 190.0630, Obs. 190.0624.

3-amino-7-methoxy-4-methyl-2*H*-chromen-2-one (**S3**). To a slurry of **S2** (866 mg, 4.55 mmol) in Ac_2O (25 mL) was added 70% HNO_3 (2.5 mL) on ice water bath slowly. After stirring on ice water bath for 20 minute, the reaction mixture was diluted with CH_2Cl_2 and

added sat. Na_2CO_3 (100 mL) carefully. The organic layer was washed with sat. Na_2CO_3 further three times (100 mL × 3). The organic layer was washed with brine and dried over Na_2SO_4. Filtration and evaporation gave a mixture of nitro isomers as yellow solid. This mixture was used for the next reaction without further purification.

A mixture of nitro isomers was suspended into MeOH (30 mL). To the slurry was added 10% Pd/C (492 mg). The inside air of the reaction flask was backfilled with H_2 gas three times. The reaction mixture was stirred at RT with an H_2 balloon overnight. The reaction mixture was filtered on Celite, and the filtrate was evaporated. The residue was purified by silica gel flash chromatography (*n*-hexane/ EtOAc = 3/2 → 1/1) gave 299 mg (32%): ^{1}H NMR ($CDCl_3$, 500 MHz, δ; ppm) 7.38 (1H, d, *J* = 8.8 Hz), 6.87 (1H, d, *J* = 2.6 Hz, 8.8 Hz), 6.83 (1H, d, *J* = 2.6 Hz), 3.85 (3H, s), 2.22 (3H, s); ^{13}C NMR ($CDCl_3$, 125 MHz, δ; ppm) 159.6, 159.4, 150.1, 127.1, 123.6, 120.6, 115.3, 112.5, 101.1, 55.9, 12.2; R_f value 0.43 (*n*-hexane/ EtOAc = 3/2); HRMS (ESI) Calcd. 205.0739, Obs. 205.0732.

1-(7-methoxy-4-methyl-2-oxo-2*H*-chromen-3-yl)-1*H*-pyrrole-2,5-dione (**Mcm-Mal**). To a solution of **S3** (148 mg, 0.721 mmol) in $CHCl_3$ (5 mL) was added maleic anhydride (72 mg, 0.734 mmol) and the reaction mixture was stirred at RT overnight. The reaction mixture was concentrated *in vacuo*. The residue was suspended into Ac_2O (7 mL) and to the reaction mixture was added NaOAc (18 mg, 0.219 mmol, 0.3 equiv.). The reaction mixture was stirred at 100 °C for 15 minutes. After cooling, the reaction mixture was diluted with AcOEt (>30 mL) and washed with sat. Na_2CO_3 (30 mL × 4). The organic layer was washed with brine and dried over Na_2SO_4. Filtration, evaporation and purification by silica gel flash chromatography (*n*-hexane/ EtOAc = 1/1 → 2/3) gave 173 mg (84%) as yellow solid: ^{1}H NMR ($CDCl_3$, 500 MHz, δ; ppm) 7.57 (1H, d, *J* = 8.9 Hz), 6.93 (1H, dd, *J* = 2.6 Hz, 8.9 Hz), 6.91 (2H, s), 6.86 (1H, d, *J* = 2.6 Hz), 3.90 (3H, s), 2.32 (3H, s); ^{13}C NMR ($CDCl_3$, 125 MHz, δ; ppm) 169.2, 163.7, 154.7, 152.9, 135.2, 126.8, 113.6, 113.3, 113.1, 101.1, 56.1, 14.7; R_f value 0.61 (*n*-hexane/ EtOAc = 1/1); HRMS (ESI) Calcd. 286.0715, Obs. 286.0704.

3-bromo-7-methoxy-4-methyl-2*H*-chromen-2-one (**Mcm-Br**). A slurry of **S2** (190 mg, 1.00 mmol), *N*-bromosuccinimide (NBS, 195 mg, 1.10 mmol, 1.1 equiv), and NH_4OAc (9 mg, 0.12 mmol, 0.1 equiv) in MeCN (5 mL) was stirred at RT for 1 h. After stirring, the reaction mixture was poured into water (20 mL) and extracted with CH_2Cl_2 (3 × 20 mL). The organic layer was washed with brine and dried over Na_2SO_4. Filtration, evaporation *in vacuo*, and purification by silica gel flash chromatography (*n*-hexane/EtOAc = 3/2 → 1/1) gave 210 mg (78%) as yellow solid: ^{1}H NMR ($CDCl_3$, 500 MHz, δ; ppm) 7.56 (1H, d, *J* = 8.5 Hz), 6.88 (1H, dd, *J* = 2.5 Hz, 8.5 Hz), 6.83 (1H, d, *J* = 2.5 Hz), 3.88 (3H, s), 2.60 (3H, s); ^{13}C NMR ($CDCl_3$, 125 MHz, δ; ppm) 162.7, 157.3, 153.5, 151.0, 125.9, 113.3, 112.9, 109.6, 100.6, 55.8, 19.4; HRMS (ESI) Calcd. 268.9808, Obs. 268.9803. Characterization matched previous reports.[1]

Synthesis of pOCNC and WpOCNC Peptides. Solid phase peptide synthesis (SPPS) of the pOCNC and WpOCNC peptides was performed on 2-chlorotrityl resin (100-200 mesh, 50 μmol scale) in a 10 mL reaction vessel. The resin was swelled in in *N,N*-dimethylformamide (DMF, 4 mL, 30 minutes) while stirring. The vessel was then drained and to it was added a Fmoc-Arg(Pbf)-OH (5 equivalents) and diisopropylethylamine (DIPEA; 10 equivalents) in DMF (2 mL). This solution was allowed to stir for 45 minutes at RT. After completion of the coupling reaction, the vessel was drained and the resin was washed with DMF (2 x 2 mL), then the coupling was repeated once more. After draining and washing the resin again, the Fmoc protecting group was removed by treatment with a 20% v/v solution of piperidine in DMF. The vessel was then drained and the resin was washed with DMF (2 x 2 mL), dichloromethane (2 x 2 mL), and DMF again (1 x 4 mL). All subsequent Fmoc deprotections were performed using this method. All subsequent amino acid (Fmoc-Aa-OH) coupling reactions were performed by using a solution of Fmoc-Aa-OH (5 equivalents), 2-(1*H*-benotriazol-1-yl)-1,1,3,3-tetramethyluronium

hexafluorophosphate (HBTU; 5 equivalents), and DIPEA (10 equivalents) in DMF (2 mL). After the last Fmoc group was removed, the resin was washed with DMF, followed by DCM (2 x 4 mL each). The resin was then dried for 30 minutes under vacuum. A cleavage cocktail (2 mL total volume) was prepared with 95:2.5:2.5 of trifluoracetic acid (TFA): triisopropyl silane (TIPS):H_2O. This was added to the resin and allowed to stir at RT for 1 hour before being drained and collected. DCM (3 mL) was added to the resin to wash out any remaining peptide and the collected solution was dried under rotary evaporation. The crude peptide product was then precipitated by adding cold diethyl ether (15 mL) and vortexing vigorously. The precipitate was pelleted by centrifugation and the ether supernatant was discarded. The resulting precipitate was dried and stored at -20 °C until HPLC purification could proceed.

HPLC Purification of Peptides. The crude precipitate from above was dissolved in 30 % v/v acetonitrile in H_2O with 0.1 % TFA (10 mL). Purification was performed by reverse phase HPLC on a Grace Vydac C18 Preparatory column (12 mL/min flow rate) using the binary gradient described in Table S1. Fractions were collected and the product peak identified by MALDI-MS (see Table S2). The collected fractions were frozen in liquid N_2 and lyophilized to white powder. The resulting solid was redissolved in 30 % v/v acetonitrile in H_2O with 0.1 % TFA (5 mL). Each peptide was subjected to a second pass of reverse phase HPLC purification using the same gradient as the first pass. The collected fractions were frozen in liquid N_2 and lyophilized to white powder for use in CaM binding experiments as follows.

Table S1. CaM binding peptide sequences and observed masses.

Peptide	Peptide Sequence	Calcd. m/z $[M+H]^+$	Obs. m/z
pOCNC	H_2N-FRRIARLVGVLREFAFR-OH	2107.5	2107.1
WpOCNC	H_2N-WRRIARLVGVLREFAFR-OH	2146.6	2147.3

Characterization of Mcm-Mal and Mcm-Br

Determination of Mcm-Mal Extinction Coefficient. Mcm-Mal, Ac-Cys and Mcm-AcOH (~2 mg) were weighted on an analytical balance. Mcm-Mal and Mcm-AcOH were dissolved in 100 μL DMSO while Ac-Cys was dissolved in 900 μL 20 mM Tris 100 mM NaCl pH 7.5. Mcm-Mal was reacted with a 100-fold excess of Ac-Cys (resulting solutions < 1 % DMSO) and allowed to react for 6 hour. Following reaction, multiple dilutions were prepared of Mcm-Mal + Ac-Cys and Mcm-AcOH and the UV-Vis absorbance of each sample was measured. The absorbance at 325 nm of each sample was plotted as function of concentration based on mass calculation and fit to a line with the extinction coefficient determined by the slope ($\varepsilon_{Mcm\text{-}AcOH} = 14440\ M^{-1}\ cm^{-1}$, $\varepsilon_{Mcm\text{-}Mal} = 19010\ M^{-1}\ cm^{-1}$).

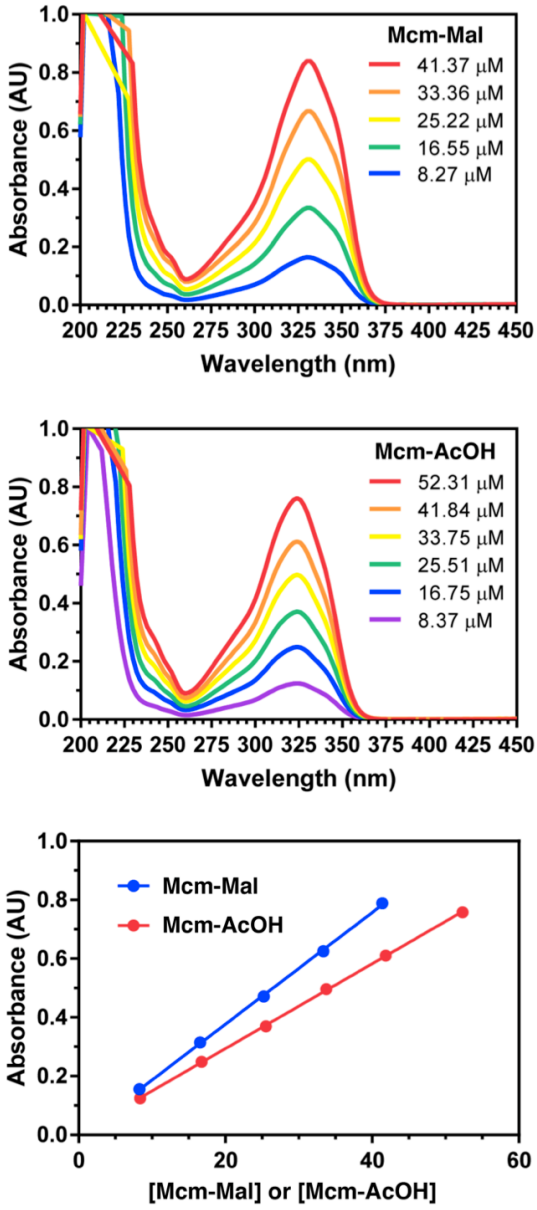

Fig. S1 Determination of Extinction Coefficient for Mcm-Mal. Top: Absorbance spectra of varying concentration of Mcm-AcOH in 20 mM Tris 100 mM NaCl pH 7.5. Middle: Absorbance spectra of varying concentration of Mcm-Mal + Ac-Cys in 20 mM Tris 100 mM NaCl pH 7.5. Bottom: Absorbance at 325 nm for varying concentrations of Mcm-Mal + Ac-Cys and Mcm-AcOH in 20 mM Tris 100 mM NaCl pH 7.5, with linear correlation for determination of extinction coefficient.

Reactions of Cys and Ac-Cys Monitored by UV/Vis, Fluorescence, and LCMS. Stocks of Mcm-Mal and Mcm-Br were prepared in DMSO and stocks of Cys and Ac-Cys were prepared in 100 mM Tris pH 7.0 or 20 mM Tris 100 mM NaCl pH 7.5, respectively. Mcm-Mal and Mcm-Br were mixed with buffer, Cys, or Ac-Cys to final concentrations of 10 μM of both Mcm derivative and Cys/Ac-Cys for UV-Vis absorbance, steady-state fluorescence and LRMS measurements. Reactions were allowed to take place for 6 hours following vortexing for 10 seconds prior to measurement. Mcm-Br $[M+H]^+$ Calcd. 269.0/271.0, Obs. 269.0/271.0; Mcm-Mal $[M+H]^+$ Calcd. 286.1, Obs. 286.2; Mcm-Mal + Cys (**S4** or **S5**) $[M+H]^+$ Calcd. 407.1, Obs. 407.2; Mcm-Mal + Ac-Cys (**S6**) $[M+H]^+$ Calcd. 449.1, Obs. 449.4

Fluorescence measurements were obtained using the PTI Quantamaster in 20 mM Tris, 100 mM NaCl pH 7.5 buffer with an excitation wavelength of 325 nm, measuring the emission from 350-450 nm, with 2 nm excitation and emission slit widths, a step size of 1 nm, and an integration time of 0.25 seconds per step.

Reaction Timecourses of Cys and Ac-Cys Monitored by Fluorescence. For timecourse measurements, 2 μM dilutions were prepared for all components from DMSO stocks of Mcm-Br/Mcm-Mal and stocks of Cys and Ac-Cys in 20 mM Tris 100 mM NaCl pH 7.5. Buffer, Cys or Ac-Cys were added to aliquots of Mcm-Mal or Mcm-Br in a 96-well plate immediately prior to measurement in a Tecan M1000 plate reader producing final concentrations of 1 μM for all reaction components. Samples were excited at 325 nm and measured and the emission was monitored at 400 nm with excitation and emission slit widths of 5 nm. Measurements were taken every 20 seconds.

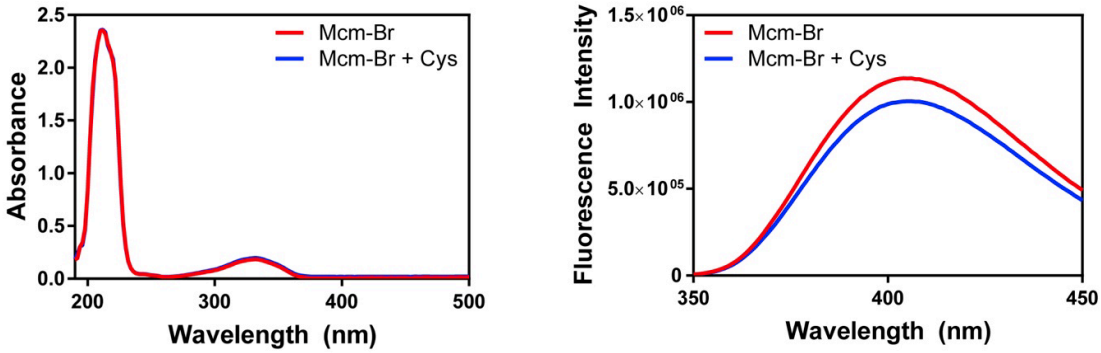

Fig. S2 Absorbance and Fluorescence Spectra of Mcm-Br. Left: Absorbance Spectra: 10 μM Mcm-Br in Tris buffer (100 mM, pH 7.0, DMSO 1%) alone, or mixed with 10 μM Cys. Right: Fluorescence Spectra: 10 μM Mcm-Br in Tris buffer (100 mM, pH 7.0, DMSO 1%) alone, or mixed with 10 μM Cys. Fluorescence excitation at 330 nm, emission monitored at 390 nm.

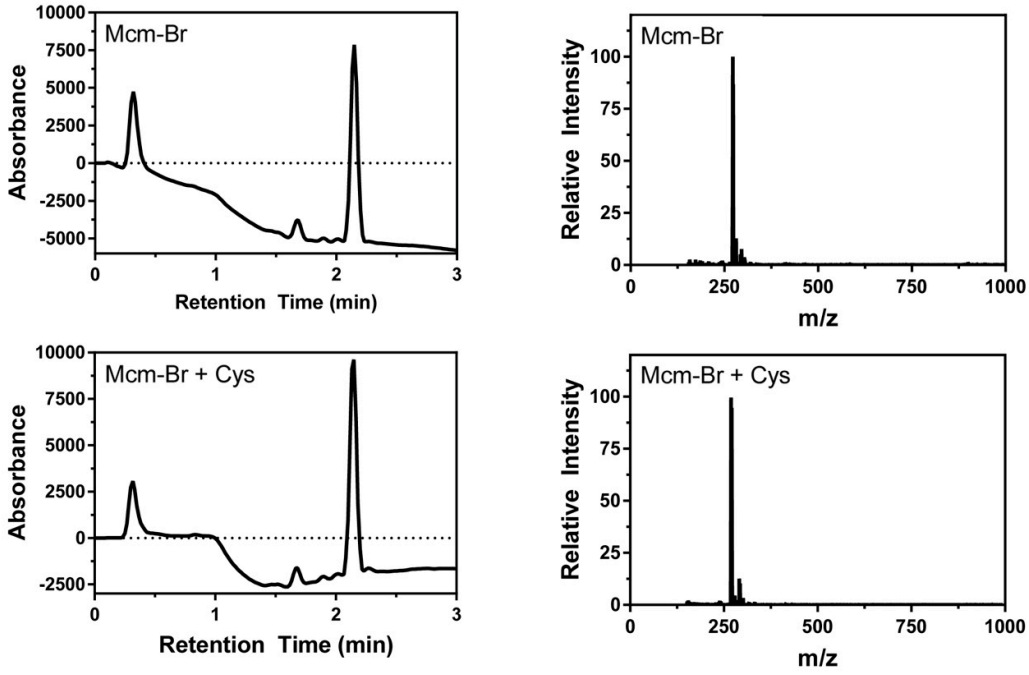

Fig. S3 LCMS Analysis of Mcm-Br Reactions with Cys. 10 μM Mcm-Br or Mcm-Mal in Tris buffer (100 mM, pH 7.0, DMSO 1%) alone or mixed with 10 μM Cys. LC chromatogram monitored at 330 nm. MS spectrum obtained for largest peak in LC chromatogram.

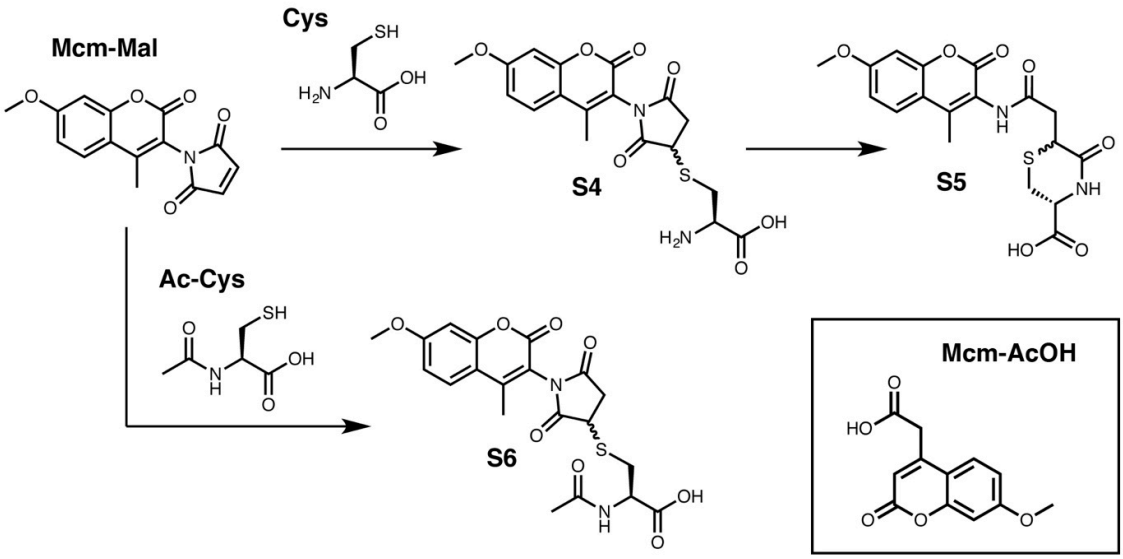

Scheme S2. Mcm-Mal Reactions with Cys and Ac-Cys and assigned products. Inset: Mcm-AcOH.

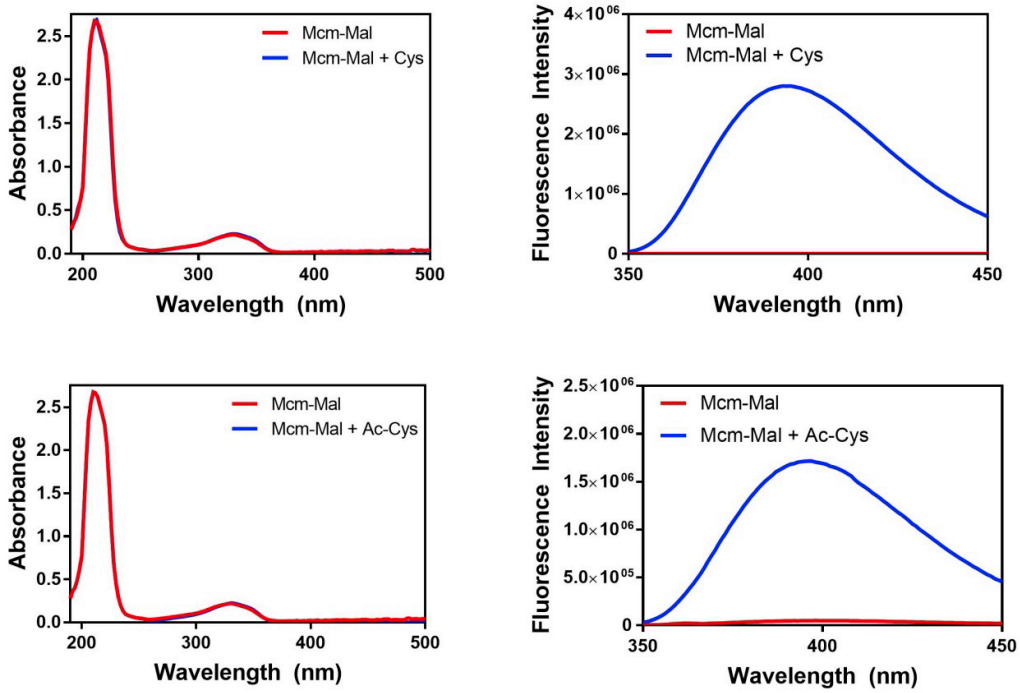

Fig. S4 Absorbance and Fluorescence Spectra of Mcm-Mal. Left: Absorbance Spectra: 10 μM Mcm-Mal in Tris buffer (10 mM, pH 7.0, DMSO 1%) alone, or mixed with 10 μM Cys or Ac-Cys. Right: Fluorescence Spectra: 10 μM Mcm-Mal in Tris buffer (100 mM, pH 7.0, DMSO 1%) alone, or mixed with 10 μM Cys or Ac-Cys.

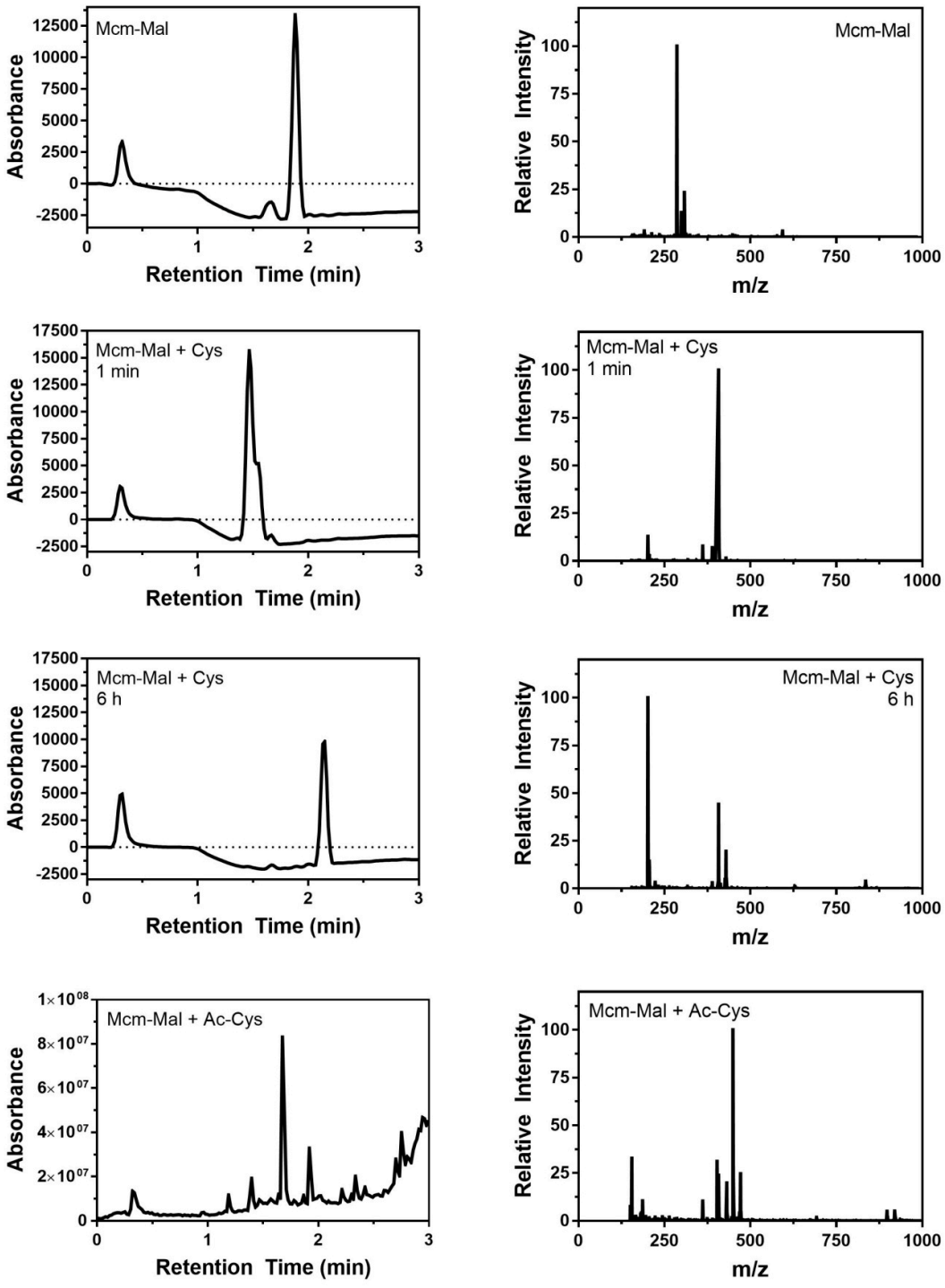

Fig. S5 LCMS Analysis of Mcm-Mal Reactions with Cys and Ac-Cys. 10 μM Mcm-Mal in Tris buffer (100 mM, pH 7.0, DMSO 1%) alone or mixed with 10 μM Cys or Ac-Cys. Cys reactions were incubated for 1 minute or 6 hours. LC chromatogram monitored at 330 nm. MS spectrum obtained for largest peak in LC chromatogram.

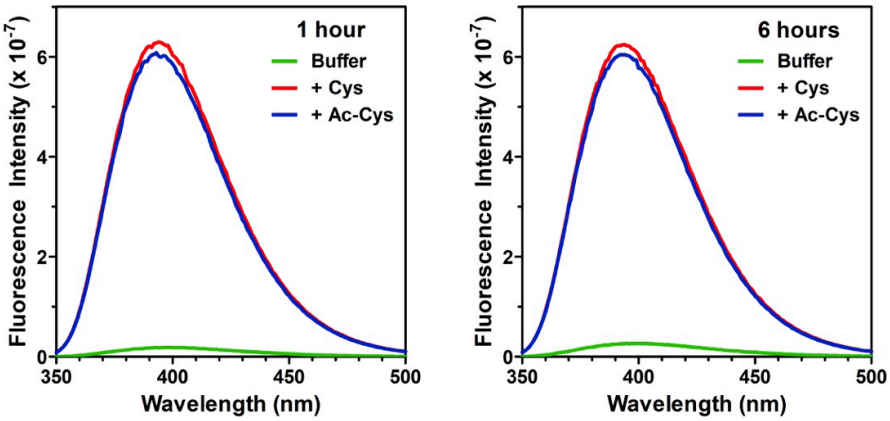

Fig. S6 Mcm-Mal Reactions with Cys and Ac-Cys after 1 and 6 h. 10 μM Mcm-Mal in Tris buffered saline (20 mM Tris, 100 mM NaCl, pH 7.5, DMSO 1%) alone or mixed with Cys or Ac-Cys. Fluorescence excitation at 325 nm, emission 350-500 nm and acquired after 1 hour (left) or 6 hours (right).

Determination of Mcm-Mal post-reaction Quantum Yield. Mcm-Mal was reacted with 10-fold excess Ac-Cys in 20 mM Tris 100 mM NaCl pH 7.5 (< 1% DMSO) for 6 hour. Six dilutions of reacted Mcm-Mal and 7-methoxycoumarin-4-yl-acetic acid (Mcm-AcOH, see Scheme S2 inset) ranging in absorbances from 0.05 to 0.02 were prepared. Fluorescence emission spectra were measured at an excitation of 325 nm over an emission range of 335 to 550 nm with 5 nm slit widths, a 1 nm step width and a 0.25 second integration time. The quantum yield was subsequently calculated for each Mcm-Mal/Mcm-AcOH pair by multiplying the quantum yield of Mcm-AcOH ($\Phi_{\text{Mcm-AcOH}} = 0.18$) by the ratio of the sum of the fluorescence emissions of Mcm-Mal to Mcm-AcOH, resulting in an average quantum yield of $\Phi_{\text{Mcm-Mal-Ac-Cys}} = 0.22$.

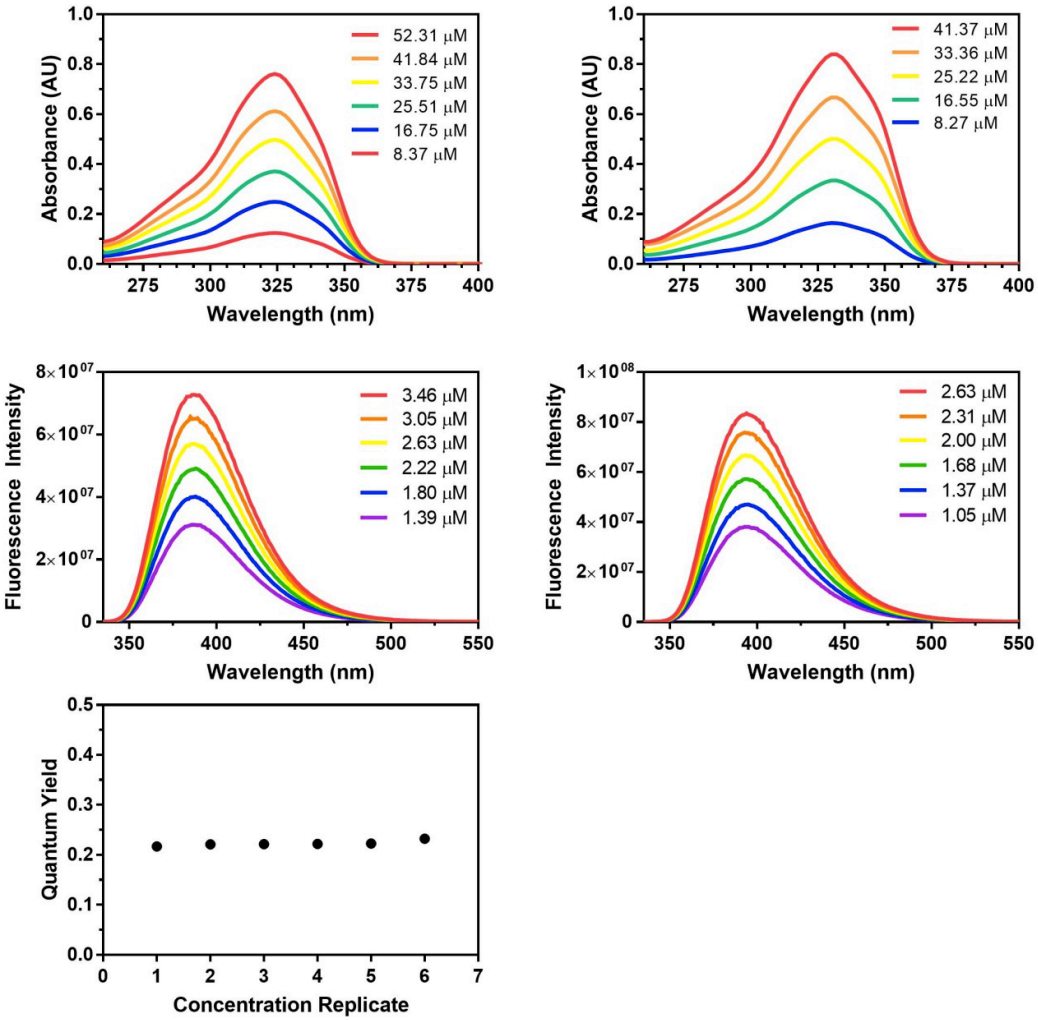

Fig. S7 Determination of Quantum Yield for Ac-Cys Mcm Product. Top left: Absorbance spectra of aliquots of Mcm-AcOH in 20 mM Tris 100 mM NaCl pH 7.5 ranging from 0.05 to 0.02. Top right: Absorbance spectra of aliquots of Ac-Cys Mcm-Mal in 20 mM Tris 100 mM NaCl pH 7.5 ranging from 0.05 to 0.02. Middle left: Fluorescence emission spectra of Mcm-AcOH dilutions in 20 mM Tris 100 mM NaCl pH 7.5 at an excitation wavelength of 325 nm. Middle right: Fluorescence emission spectra of Ac-Cys Mcm-Mal dilutions in 20 mM Tris 100 mM NaCl pH 7.5 at an excitation wavelength of 325 nm. Bottom left: Calculated quantum yield values for each sample combination.

Protein Expression, Labelling, and Purification

Cloning of CaM Constructs. The gene encoding full-length calmodulin was previously cloned into the pTXB1 vector containing a C-terminal MxeGyrA intein, followed by a His_6 purification tag.[2] A 'TAG' codon for the incorporation of Acd at Leu_{112} via amber stop codon suppression and a 'TGC' codon encoding Cys at Phe_{12} for Mcm-Mal labelling were inserted using the following sets of primers in QuikChange® PCR. In the case of the $F_{12}C$-$L_{112}\delta$ double mutant, the CaM-$F_{12}C$ mutant was obtained first, before using the TAG_{112} primers in a second round of PCR to obtain the desired plasmid.

i. Phe_{12} → Cys

Forward: 5'-GAGCAGATTGCAGAATGCAAAGAAGCTTTTTCACTA-3'

Reverse: 5'-TAGTGAAAAAGVTTVTTTGCATTCTGCAATCTGCTC -3'

ii. Leu_{112} → TAG

Forward: 5'-GCAGAACTTCGTCATGAGATGACAAATTAGGGGGAGAAGCTAACA -3'

Reverse: 3'-TGTTAGCTTCTCCCCCTAATTTGTCATCACATGACGAAGTTCTGC-3'

Expression of CaM C_{12}-GyrA-H_6. A plasmid encoding CaM $F_{12}C$-GyrA was transformed into BL21-Gold (DE3) *E. Coli* cells and grown against ampicillin (Amp, 100 μg/mL) on an LB-agar plate. Single colonies were picked and grown in liquid LB media (2 x 5 mL, 100 μg/mL ampicillin) with shaking (250 RPM) at 37 °C until saturation. Both primary cultures were then added to a secondary culture of autoclaved M9 media (500 mL, 100 μg/mL Amp) and grown at 37 °C, with shaking (250 RPM) until OD_{600}= 0.8 (3-4 h). Isopropyl β-D-1-thiogalactopyranoside (IPTG) was then added (final concentration = 1 mM) and the temperature and shaking speed were reduced to 25 °C and 225 RPM respectively for 16 h of additional incubation.

Expression of CaM-δ_{112} and CaM-$C_{12}\delta_{112}$. Plasmids encoding CaM-δ_{112}-GyrA-H_6 and CaM-$C_{12}\delta_{112}$-GyrA-H_6 were separately transformed into BL21 cells that also contain a plasmid encoding for an orthogonal Acd synthetase 2b (AcdRS2b, also referred to as clone A9) and $tRNA_{CUA}$ pair described in detail elsewhere.[2, 3] These transformations were grown against streptomycin (Strep, 100 μg/mL) and Amp (100 μg/mL) on an LB-agar plate. Single colonies were picked and grown in liquid LB media (2 x 5 mL each, 100 μg/mL each of Strep and Amp) with shaking (250 RPM) until saturation. Both primary cultures were then added to a secondary culture of autoclaved M9 media (500 mL, 100 μg/mL each of Strep and Amp) and grown at 37 °C with shaking (250 RPM) until OD_{600}=0.7 (3-4 hours). IPTG and Acd were then added (1 mM and 0.5 mM final concentrations, respectively) and the temperature and shaking speed were reduced to 18 °C and 225 RPM, respectively. These cultures were then incubated at these conditions for 20 hours.

Purification of CaM Constructs. Cells were harvested by centrifugation at 5,000 RPM in a GS3 rotor and Sorvall RC-5 centrifuge for 15 minutes at 4 °C. The supernatant was discarded and the cell pellet was suspended in 20 mL lysis buffer (50 mM HEPES, pH 7.5) containing a broad spectrum protease inhibitor tablet. Resuspended cells were then lysed on ice by sonication (30 amps power, 2 second pulse, 2 second rest, 4 minutes total sonication time) and then pelleted at 13,000 RPM in an SS-34 rotor (Sorvall RC-5 centrifuge) for 15 minutes at 4 °C. The supernatant was collected and incubated with Ni^{2+}-NTA resin (2 mL column volume) for 1 h on ice with shaking. The slurry was then added to a fritted column and the liquid was allowed to flow through. The resin was then washed with 3 x 10 mL of buffer (50 mM HEPES, pH 7.5) and 3 x 10 mL of wash buffer (50 mM HEPES, 10 mM imidazole, pH 7.5). Each CaM construct was then eluted from the resin in 5 fractions each containing 3 mL of elution buffer (50 mM HEPES, 300 mM imidazole, pH 7.5). The pooled fractions were immediately subjected to intein cleavage conditions by adding β-mercaptoethanol to a final concentration of 200 mM and incubated on a rotisserie at RT for

20 hours. The resulting cleavage solution was then dialyzed against 20 mM Tris pH 8.0 (2L) overnight in preparation for anion exchange purification via FPLC. Prior to FPLC purification, 10 μL of 0.5 M TCEP Bond Breaker™ was added to the CaM-C_{12} and CaM-$C_{12}\delta_{112}$ constructs to reduce any aberrant disulfides formed between CaM proteins and/or βME. Each CaM construct was purified over a HiTrap Q column using a 120 min NaCl gradient (0.1 M to 0.8 M NaCl in 20 mM Tris, pH 8.0). Fractions containing the product peak were confirmed by MALDI and dialyzed twice against water at 4 °C (2 L, 2 hours each). These samples were then flash frozen in liquid N_2 and lyophilized to a powder.

CaM Labelling with Mcm-Mal. A stock solution of ~25 mM Mcm-Mal was prepared by dissolving 4.6 mg of Mcm-Mal solid in 645 μL DMSO. CaM-C_{12} and CaM-$C_{12}\delta_{112}$ samples were dissolved in 1 mL of 20 mM Tris, pH 7.5. To each sample was added 10 equivalents of Mcm-Mal (based off UV-Vis quantification of protein solutions) and the samples were incubated at 37 °C with shaking (200 RPM) for 3 hours. Each sample was then diluted in 2 mL of 20 mM Tris pH 8.0 and subjected to a second round of FPLC purification using the gradient described above. Fractions were analyzed by MALDI MS and fractions containing the desired mass for Cys-Mcm conjugated product were pooled and dialyzed (2 x 2 L) against water before being flash frozen in N_2 and lyophilized to a powder.

αS-Q_{62}C and αS-E_{114}C Expression. α-Synuclein (αS) mutant plasmids (pTXB1_αS-C_{62}_Mxe-H_6 or pTXB1_αS-C_{114}_Mxe-H_6) were transformed into competent *E. coli* BL21(DE3) cells and plated on LB agar plates supplemented with Amp overnight at 37 °C.[4] Single colonies were used to inoculate 5 mL of LB media supplemented with Amp (100 μg/mL). The primary culture was incubated at 37 °C with shaking at 250 rpm for 4 h. A single primary culture was used to inoculate 1 L of LB media containing Amp (100 mg/L) which was then grown at 37 °C with shaking at 250 rpm until it reached OD ~0.7. Expression was induced with IPTG (1 mM) and the temperature was reduced to 18 °C overnight.

αS-δ_{94}, αS-$C_{62}\delta_{94}$, and αS-$\delta_{94}C_{114}$ Expression. αS mutant plasmids (pTXB1_αS-TAG_{94}_Mxe-H_6, pTXB1_αS-$C_{62}TAG_{94}$_Mxe-H_6, or pTXB1_αS-$TAG_{94}C_{114}$_Mxe-H_6, generated using plasmids in Haney *et al*.) and an AcdRS2b/ tRNA plasmid were transformed into competent *E. coli* BL21(DE3) cells and plated on LB agar plates supplemented with Amp overnight at 37 °C.[3, 5] Single colonies were used to inoculate 5 mL of LB media supplemented with Amp and streptomycin (Strep, 100 μg/mL of each). The primary culture was incubated at 37 °C with shaking at 250 rpm for 4 h. A single primary culture was used to inoculate 1 L of LB media containing Amp and Strep (100 mg/L) which was grown at 37 °C with shaking at 250 rpm until it reached OD ~0.7. Expression was induced by adding IPTG and Acd (concentrations of 1 mM and 140 mg/L, respectively) which was then incubated overnight at 18 °C with shaking at 250 rpm.

Purification of αS Constructs. Cells were harvested by centrifugation at 4,000 RPM in a GS3 rotor and Sorvall RC-5 centrifuge for 20 minutes at 4 °C. The supernatant was discarded and the cell pellet was suspended in 15 mL lysis buffer (40 mM Tris, 5 mM EDTA, pH 8.0) containing one Roche protease inhibitor cocktail pill (cOmplete mini tablets, EDTA-free, Easy Pack, Roche Cat. #04693159001). Resuspended cells were then lysed on ice by sonication (30 amps power, 1 second pulse, 1 second rest, 5 minutes total sonication time) and then pelleted at 14,000 RPM in an SS-34 rotor (Sorvall RC-5 centrifuge) for 20 minutes at 4 °C. The supernatant was collected and incubated with Ni^{2+}-NTA resin (3 mL column volume) for 1 h on ice with shaking. The slurry was then added to a fritted column and the liquid was allowed to flow through. The resin was then washed with 3 x 5 mL of buffer (50 mM HEPES, pH 7.5) and 2 x 10 mL of wash buffer (50 mM HEPES, 10 mM imidazole, pH 7.5). Constructs were then eluted from the resin in 4 fractions each containing 3 mL of elution buffer (50 mM HEPES, 300 mM imidazole, pH 7.5). The pooled fractions were immediately subjected to intein cleavage conditions by adding β-mercaptoethanol to a final concentration of 200 mM and incubated on a rotisserie at RT for

20 hours. The resulting cleavage solution was then dialyzed against 20 mM Tris pH 8.0 overnight. Prior to FPLC purification, 10 μL of 0.5 M TCEP Bond Breaker™ was added to the Cys constaining constructs to reduce any aberrant disulfides formed between αS proteins and/or βME. Each construct was purified by ion-exchange chromatography using a HiTrap Q HP column (5 mL) on an ÄKTA FPLC using a 100 minutes NaCl gradient (0 to 500 mM NaCl in 20 mM Tris, pH 8.0). The fractions containing the product were identified by MALDI MS. αS-δ_{94} mutant was dialyzed at 4 °C against αS buffer (20 mM Tris, 100 mM NaCl, pH 7.5) overnight and stored at −80 °C in 1.5 mL aliquots and thawed once for experiments. Cys containing mutants were carried directly into the labelling step following purification.

αS Labelling with Mcm-Mal. The protein solution after FPLC (ca. 10–20 mL) was treated with 20 μL Bond Breaker solution. To the protein solution was added 25 mM Mcm-Mal solution in DMSO (200–300 μL). Each reaction step was monitored by MALDI MS. After labelling with Mcm-Mal, the solution was dialyzed at 4 °C against Tris buffer (20 mM, pH 8.0) overnight. The dialyzed solution was concentrated by centrifugation with a 3 kDa cutoff filter (milliporesigma #UFC900324). The concentrated solution was purified by HPLC with a protein C4 column (Vydac #214TP1010). After concentration by centrifugation with a 3 kDa cutoff filter, the solution was dialyzed against αS buffer (20 mM Tris, 100 mM NaCl, pH 7.5) overnight. Following dialysis, αS in buffer was stored at −80 °C in 1.5 mL aliquots and thawed once for experiments.

Table S2. Protein MALDI Masses.

Protein	Calc. $[M+H]^+$or $[M+Na]^+$	Obs. $[M+H]^+$or $[M+Na]^+$
αS-C^{Mcm}_{62}	14721	14731
αS-$C^{Mcm}_{62}\delta_{94}$	14838	14844
αS-C^{Mcm}_{114}	14720	14727
αS-$\delta_{94}C^{Mcm}_{114}$	14837	14844
αS-δ_{94}	14757	14757
CaM-C^{Mcm}_{12}	16950	16947
CaM-δ_{112}	16881	16889
CaM-$C^{Mcm}_{12}\delta_{112}$	17123	17133

Table S3. Trypsin Fragment MALDI Masses.

Protein	Fragment	Calc. $[M+H]^+$	$[M + Na]^+$	Obs. $[M+H]^+$	$[M+Na]^+$
αS-C^{Mcm}_{62}	61-80	2207	2229	2206	2228
αS-$C^{Mcm}_{62}\delta_{94}$	61-80	2207	2229	2206	2228
	81-96	1596	1618	1595	1618
αS-C^{Mcm}_{114}	103-140	4564	4586	4562	4584
αS-$\delta_{94}C^{Mcm}_{114}$	81-96	1596	1618	1596	1618
	103-140	4564	4586	4561	4564
αS-δ_{94}	81-96	1596	1618	1596	1618
CaM-C^{Mcm}_{12}	1-13	1763	1785	1761	1783
CaM-δ_{112}	107-115	1179	1201	1180	1201
CaM-$C^{Mcm}_{12}\delta_{112}$	1-13	1763	1785	1762	1784
	107-115	1179	1201	1179	1201

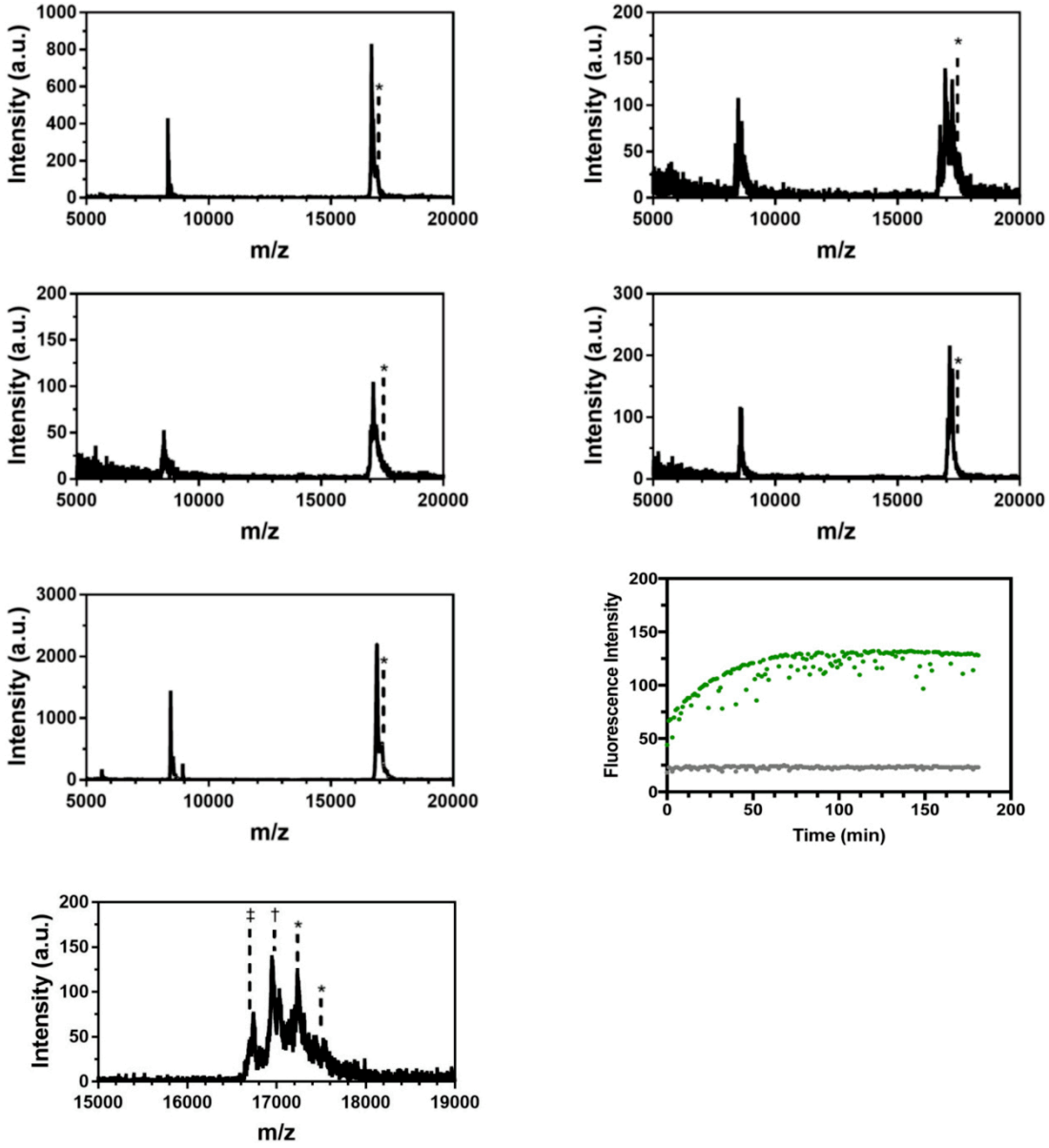

Fig. S8 MALDI MS Characterization of CaM Variants. On each plot matrix adduct peaks are marked with * The plots show CaM-C_{12} (First Row Left), CaM-$C^{Mcm}{}_{12}$ (First Row Right), CaM-$C_{12}\delta_{112}$ (Second Row Left), CaM-$C^{Mcm}{}_{12}\delta_{112}$ (Second Row Right) and CaM-δ_{112} (Third Row Left). An enlarged spectrum of the region of interest for the CaM-$C^{Mcm}{}_{12}\delta_{112}$ shown where the labeled and unlabeled protein masses are indicated with † and ‡ respectively (Fourth Row Left). Fluorescence emission at 390 nm from excitation at 325 nm was monitored after mixing 35 μM CaM-C_{12} with 3 equiv Mcm-Mal in Tris buffer, pH 7.5 (Third Row Right, Green: CaM-C_{12}, Grey: Buffer control).

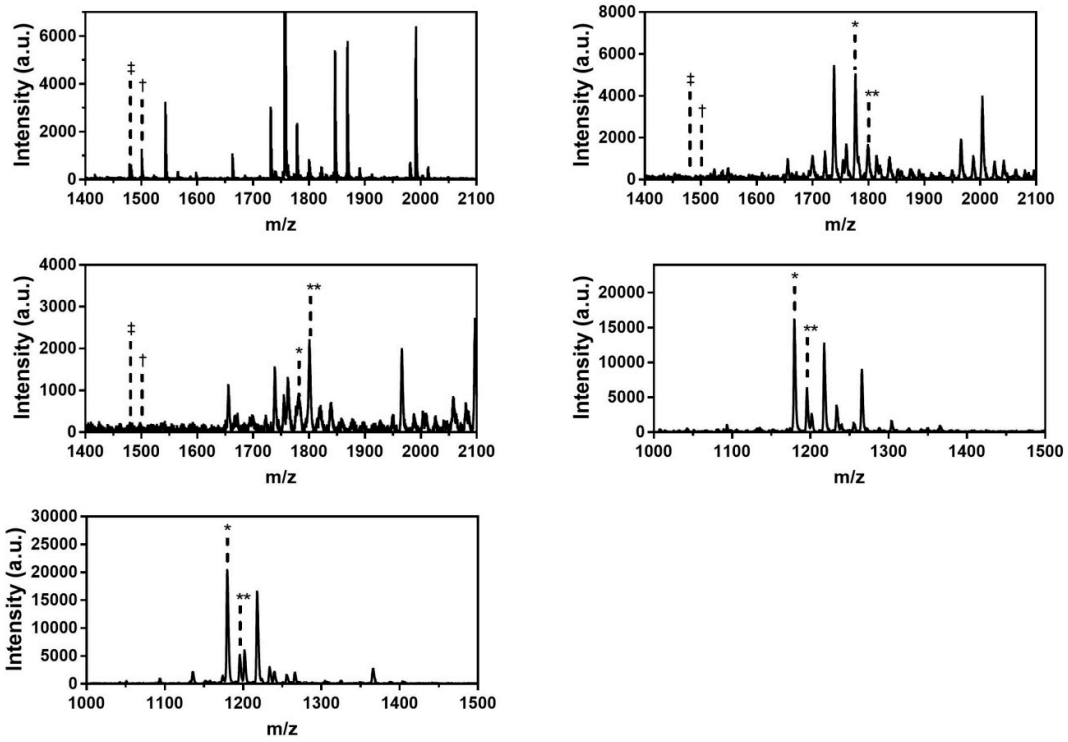

Fig. S9 Trypsin Digest MALDI MS Characterization of CaM Variants. On each plot, the M+H peak of the fragment of interest is marked with * and the M+Na peak is marked with **, while the M+H peak corresponding to unlabeled Cys containing protein is denoted with ‡ and the M+Na peak is marked with †.. The plots show the fragments of $CaM_{1\text{-}13}\text{-}C_{12}$ of CaM-C_{12} (Top Left), $CaM_{1\text{-}13}\text{-}C^{Mcm}{}_{12}$ of CaM-$C^{Mcm}{}_{12}$ (Top Right), $CaM_{1\text{-}13}\text{-}C^{Mcm}{}_{12}$ of CaM-$C^{Mcm}{}_{12}\delta_{112}$ (Middle Left) and $CaM_{107\text{-}115}\text{-}\ \delta_{112}$ of CaM-$C^{Mcm}{}_{12}\delta_{112}$ (Middle Right), $CaM_{107\text{-}115}\text{-}\delta_{112}$ of CaM-δ_{112} (Bottom Left),.

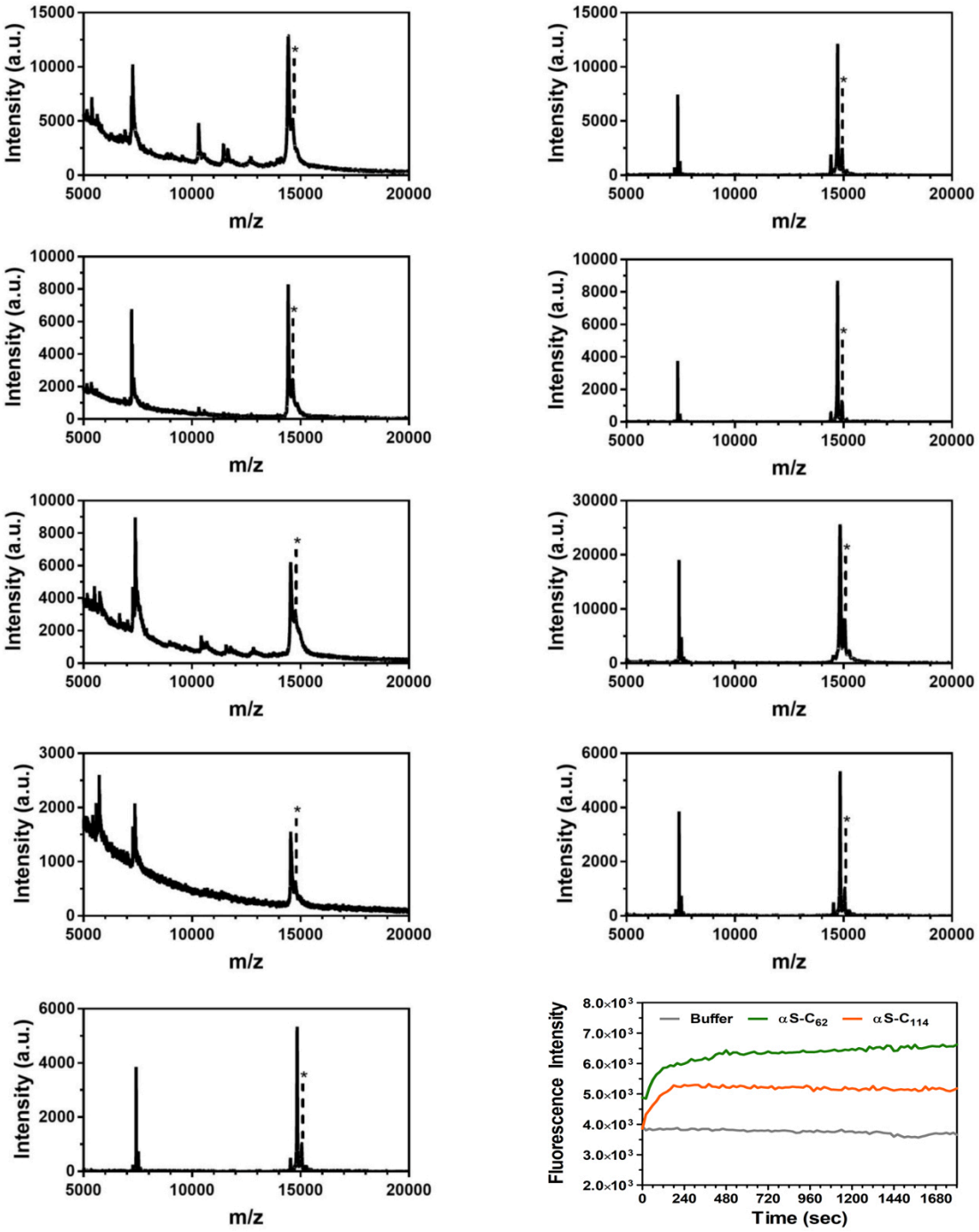

Fig. S10 MALDI MS Characterization of αS Variants. On each plot matrix adduct peaks are marked with *. The plots show αS-C_{62} (Row 1 Left), αS-C^{Mcm}_{62} (Row 1 Right), αS-C_{114} (Row 2 Left), αS-C^{Mcm}_{114} (Row 2 Right), αS-$C_{62}\delta_{94}$ (Row 3 Left), αS-$C^{Mcm}_{62}\delta_{94}$ (Row 3 Right), αS-$\delta_{94}C_{114}$ (Row 4 Left), αS-$\delta_{94}C^{Mcm}_{114}$ (Row 4 Right) and αS αS-δ_{94} (Row 5 Left). Fluorescence emission at 400 nm from excitation at 325 nm was monitored after mixing 1 μM αS-C_{62} or αS-C_{114} with 1 equiv Mcm-Mal in 20 mM Tris buffer, pH 7.5 (Bottom Right, Green: αS-C_{62}, Orange: αS-C_{114}, Grey: Buffer control).

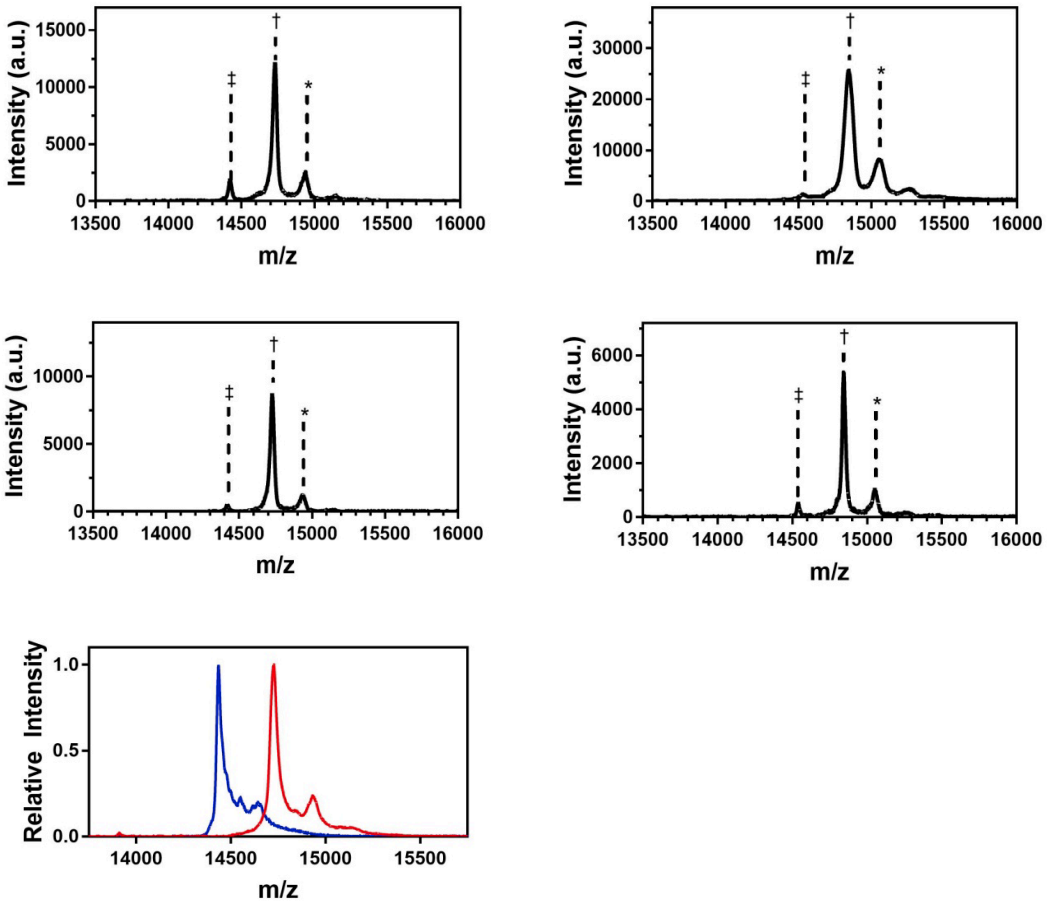

Fig. S11 Enlarged MALDI MS of labeled αS Variants. Spectra where the region of interest is enlarged for αS-C^{Mcm}_{62} (Top Left), αS-$C^{Mcm}_{62}\delta_{94}$ (Top Right), αS-C^{Mcm}_{114} (Middle Left) and αS-$\delta_{94}C_{114}$ (Middle Right) where the labeled and unlabeled protein masses are indicated with † and ‡ respectively. MALDI MS of αS-C^{Mcm}_{62} before (blue) and after 3 hr labeling reaction (red) showing extend of labeling (Bottom Left).

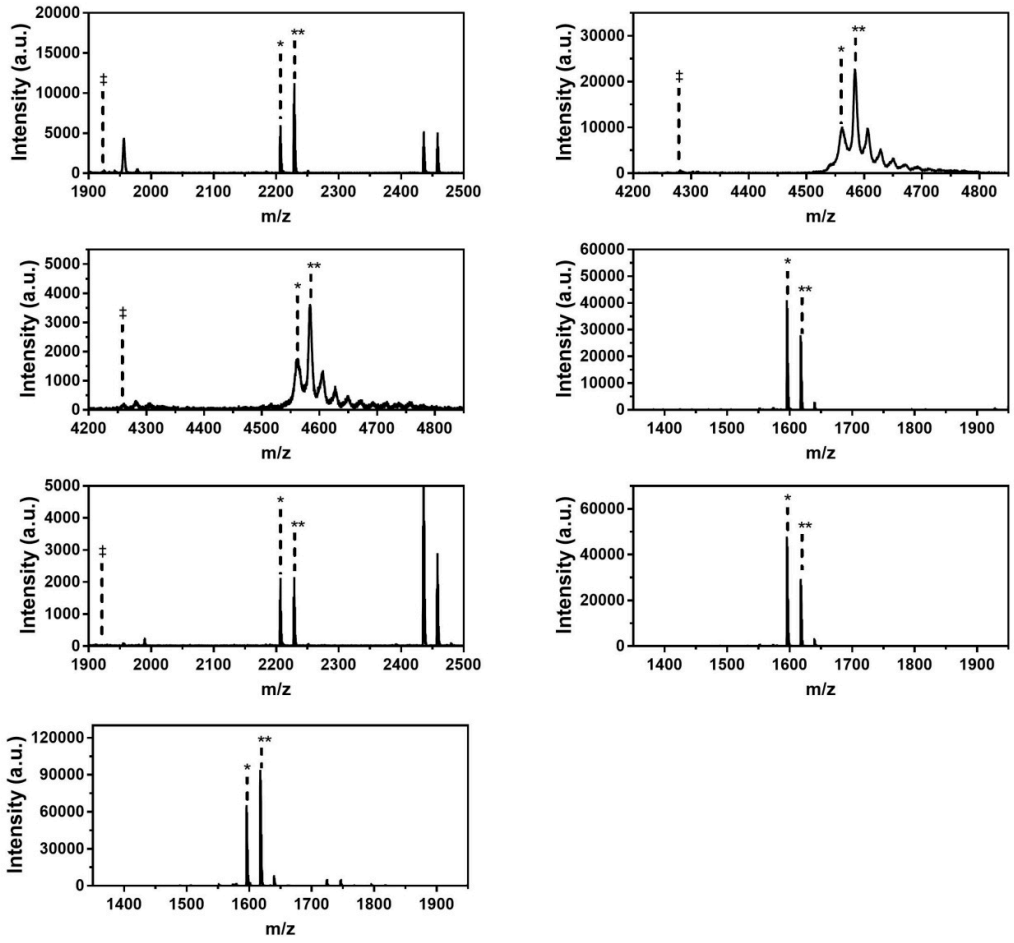

Fig. S12 Tryspin Digest MALDI MS Characterization of αS Variants. On each plot, the M+H peak of the fragment of interest is marked with * and the M+Na peak is marked with **. The mass corresponding to unlabeled Cys containing protein is denoted with ‡. The plots show the fragments $\alpha S_{61\text{-}80}\text{-}C^{Mcm}{}_{62}$ of αS-$C^{Mcm}{}_{62}$ (Top Left), $\alpha S_{103\text{-}140}\text{-}C^{Mcm}{}_{114}$ of αS-$C^{Mcm}{}_{114}$ (Top Right), $\alpha S_{103\text{-}140}\text{-}C^{Mcm}{}_{114}$ of αS-$\delta_{94}C_{114}$ (Upper Middle Left), $\alpha S_{81\text{-}94}$- δ_{94} of αS-$\delta_{94}C_{114}$ (Upper Middle Right), $\alpha S_{61\text{-}80}\text{-}C^{Mcm}{}_{62}$ of αS-$C^{Mcm}{}_{62}\delta_{94}$ (Bottom Middle Left), $\alpha S_{81\text{-}94}\text{-}\delta_{94}$ of αS-$C^{Mcm}{}_{62}\text{-}\delta_{94}$ (Bottom Middle Right), and $\alpha S_{81\text{-}94}\text{-}\delta_{94}$ of αS-δ_{94} (Bottom Left).

FRET Calculations

For FRET measurements, the Förster distance, R_0, is given in Å by Equation (S1)

$$R_0^6 = \frac{9000(\ln 10)\kappa^2 \Phi_D J}{128\pi^5 n^4 N_A} \quad \text{(S1)}$$

where κ^2 is a geometrical factor that relates the orientation of the donor and acceptor transition moments, Φ_D is the quantum yield of the donor, n is the index of refraction of the solvent, N_A is Avogadro's number, and J is the spectral overlap integral defined in units of $M^{-1}\bullet cm^{-1}\bullet nm^4$. J is formally defined as

$$J = \int_0^\infty f_D(\lambda)\varepsilon_A(\lambda)\lambda^4 \, d\lambda \quad \text{(S2)}$$

where $\varepsilon_A(\lambda)$ is the molar extinction coefficient of the acceptor at each wavelength λ and $f_D(\lambda)$ is the normalized donor emission spectrum given by

$$f_D(\lambda) = \frac{F_{D\lambda}(\lambda)}{\int_0^\infty F_{D\lambda}(\lambda) d\lambda} \quad \text{(S3)}$$

where $F_{D\lambda}(\lambda)$ is the fluorescence of the donor at each wavelength λ. Substituting these results into Equation (S1), as well as the donor (Mcm) quantum yield, 1.33 for the index of refraction of water, and 2/3 for κ^2 gives the Förster distance. These R_0 values were used to calculate FRET efficiency (E_{FRET}) as a function of distance using Equation (S4).

$$E_{FRET} = \frac{1}{1 + \left(\frac{R}{R_0}\right)^6} \quad \text{(S4)}$$

Here, E_{FRET} is the FRET efficiency and R is the separation between the chromophores. These values are reported in Table S4.

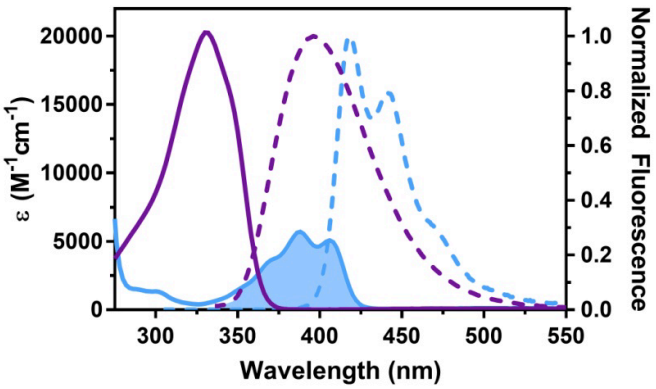

Fig. S13 Ac-Cys^{Mcm} and Acd Absorption and Emission Spectra. Ac-Cys^{Mcm} (puple) and Acd (blue) absorption spectra (solid lines) were measured in 20 mM Tris 100 mM NaCl, pH. 7.5. Ac-Cys^{Mcm} (purple) and Acd (blue) fluorescence emission spectra (dashed lines) were measured with excitation at 325 nm for Ac-Cys^{Mcm} and 386 nm for Acd. Spectral overlap between Ac-Cys^{Mcm} emission and Acd absorption is indicated by the shaded area.

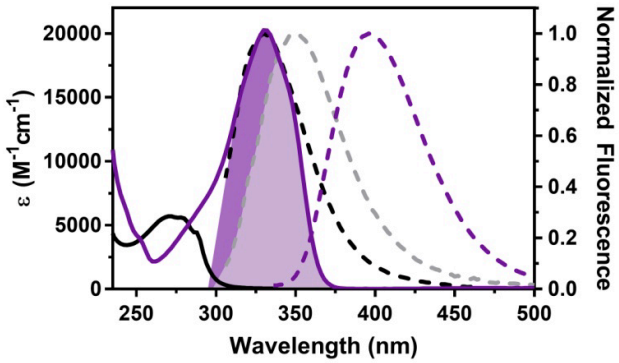

Fig. S14 Trp and Ac-Cys^{Mcm} Absorption and Emission Spectra. Ac-Cys^{Mcm} (purple) and Trp (black) absorption spectra (solid lines) were measured in 20 mM Tris 100 mM NaCl, pH. 7.5. Ac-Cys^{Mcm} (purple) and Trp (black or grey) fluorescence emission spectra (dashed lines) were measured with excitation at 325 nm for Mcm-Mal and 295 nm for Trp in the WpOCNC peptide in the absence (black) and presence (grey) of wild-type CaM to illustrate the change in overlap due to solvation environment. Spectral overlap between Trp emission and Ac-Cys^{Mcm} absorption is indicated by the shaded areas.

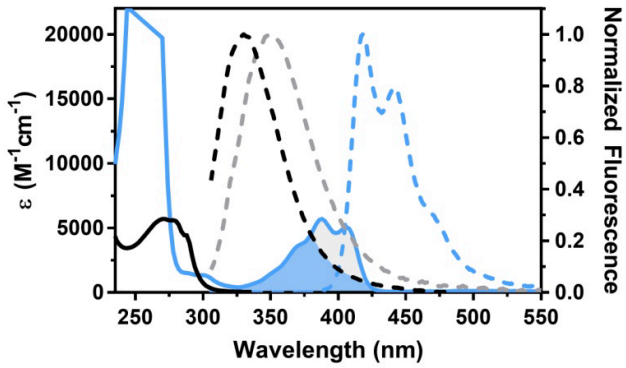

Fig. S15 Trp and Acd Absorption and Emission Spectra. Trp (black) and Acd (blue) absorption spectra (solid lines) were measured in 20 mM Tris 100 mM NaCl, pH. 7.5. Trp (black and grey) and Acd (blue) fluorescence emission spectra (dashed lines) were measured with excitation at 386 nm for Acd and 295 nm for Trp in the WpOCNC peptide in the absence (black) and presence (grey) of wild-type CaM to illustrate the change in overlap due to solvation environment. Spectral overlap between Trp emission and Acd absorption is indicated by the shaded areas.

CaM FRET Measurements

Steady-State Fluorescence Measurements. Following preparation, dried CaM mutants along with pOCNC and WpOCNC peptides were re-dissolved in 15 mM HEPES, 140 mM KCL, and 6 mM $CaCl_2$, pH 6.70. Concentrations of CaM mutants were determined based on Mcm (ε_{Mcm325} = 19010 $M^{-1}cm^{-1}$) or Acd (ε_{Acd386} = 5700 $M^{-1}cm^{-1}$) absorbance while pOCNC and WpOCNC peptide concentrations were determined based on Phe (ε_{Phe259} = 189 $M^{-1}cm^{-1}$) or Trp (ε_{Trp276} = 5579 $M^{-1}cm^{-1}$) absorbance. Fluorescence measurements were taken on a PTI QuantaMaster 40 system. Trp emission spectra were collected with an excitation wavelength at 295 nm over an emission range of 305-600 nm, Mcm emission spectra were collected with an excitation wavelength at 325 nm over an emission range of 335-600 nm, and Acd emission spectra were collected with an excitation wavelength at 386 nm over an emission range of 396-600 nm. All spectra were collected with excitation and emission wavelengths set to 5 nm with a 0.25 second integration time and a 1 nm step size. CaM mutants were measured at a concentration of 0.5 μM in the absence of peptide, and the presence of pOCNC or WpOCNC peptide at a concentration of 1 μM. A single control measurement to determine the fluorescence spectrum of the bound WpOCNC peptide was taken at a 1 μM concentration of peptide and a 2 μM concentration of wild-type CaM.

Table S4. CaM + WpOCNC FRET

	Φ_D	J (M^{-1}•cm^{-1}•nm^4)	R_0 (Å)	E_{FRET}	Distance (Å)
Free	0.16	7.042 x 10^{13}	24.6	0.676 ± 0.002	25.9 ± 0.1
Bound	0.17	7.137 x 10^{13}	24.3	0.405 ± 0.001	21.8 ± 0.1

Determination of Peptide Binding Affinity. To confirm that the binding affinity of CaM was not perturbed by the introduction of fluorescent probes, the binding affinity was determined for CaM-$C^{Mcm}{}_{12}\delta_{112}$. This was performed by mixing labeled and wild-type CaM in varied concentrations with 1 μM WpOCNC at concentration ratios of 0.125:1, 0.25:1, 0.5:1,

1:1 and 1.5:1 of protein to peptide. Trp emission specta were collected as previously described. For the wild-type protein, the wavelength of the maximum of the Trp fluorescence was used to quantitatively determine the amount of bound peptide, while for CaM-$C^{Mcm}{}_{12}\delta_{112}$ the amount of bound protein was determined via the quenching in the emission at 350 nm. The normalized values were then fit with Equation (S5) to determine Kd as in previous publications.[6]

$$y = R\frac{(K_d + [P] + [P][L]) - \sqrt{(K_d + [P] + [P][L])^2 - 4[P]^2[L]}}{2[P]} \qquad \text{(S5)}$$

In Equation (S5) [P] and [L] are the total concentrations of the protein and peptide respectively The K_d for the wild-type and CaM-$C^{Mcm}{}_{12}\delta_{112}$ proteins were 7.44±6.89 and 21.8±20.5 nM respectively. Given the high affinity of the WpOCNC peptide and the 1 μM concentration in our assay, these represent only estimates of the actual K_d, with significant error. However, we take the stoichiometric binding observed in both cases to indicate that CaM labeling does not substantially disrupt peptide binding.

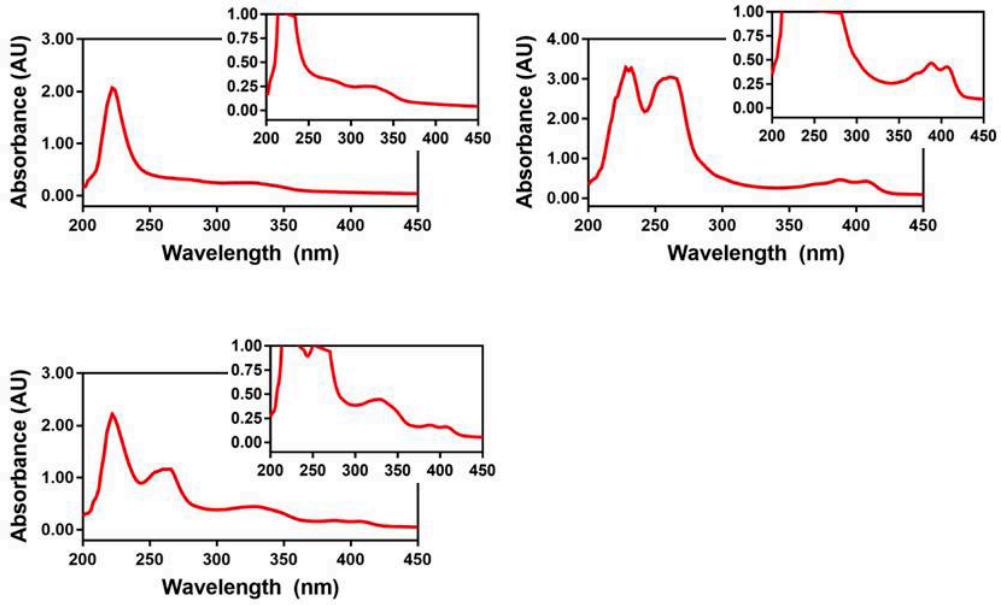

Fig. S16 CaM Absorbance Measurements. Absorbance spectra of CaM-$C^{Mcm}{}_{12}$ (Top Left), CaM-δ_{112} (Top Right) and CaM-$C^{Mcm}{}_{12}\delta_{112}$ (Bottom Left)

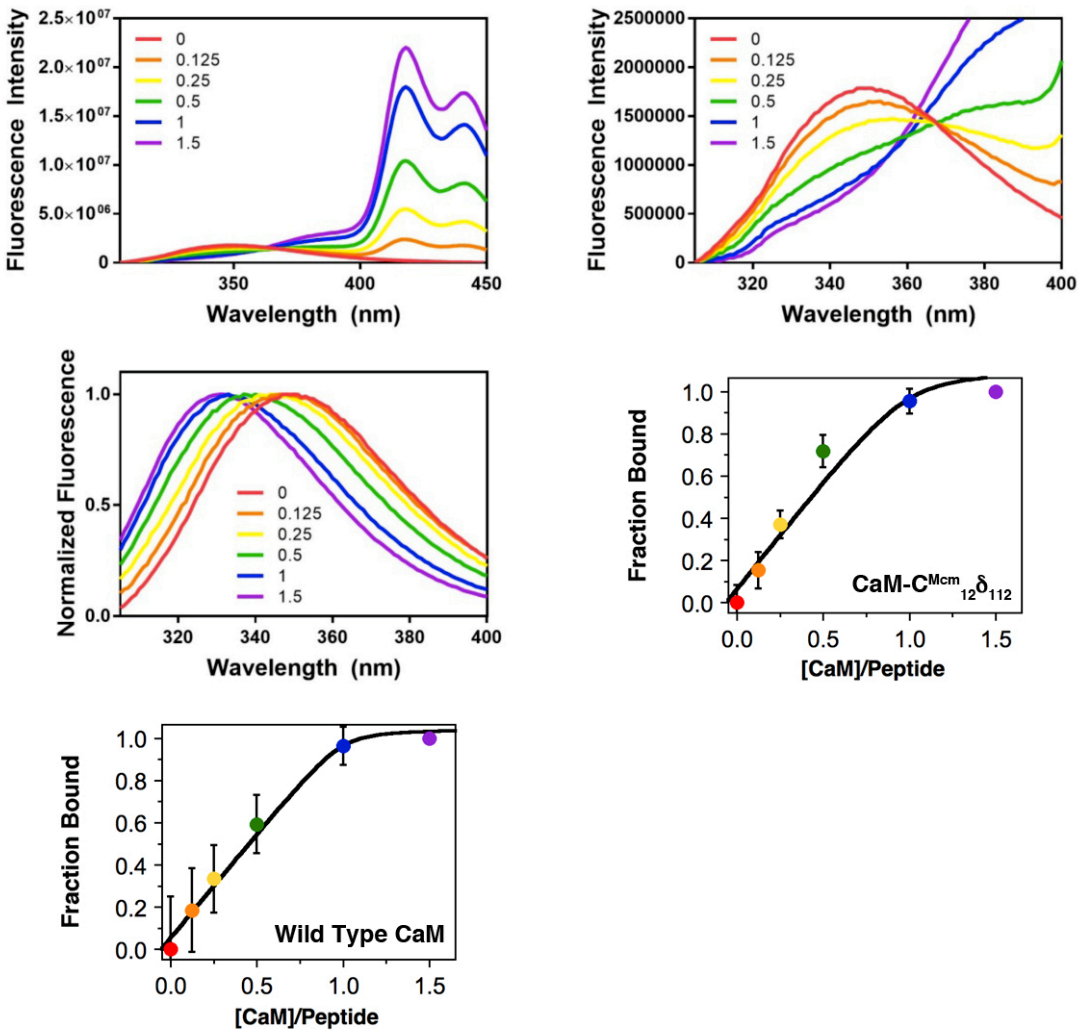

Fig. S17 Fluorescence Assay to Determine Binding of Labeled CaM. Fluorescence spectra of WpOCNC binding to CaM-$C^{Mcm}_{12}\delta_{112}$ (Top Left and Right) and CaM-WT (Middle Left) with the relative concentration of CaM:WpOCNC indicated in the legend. Plots of fraction of WpOCNC bound for both CaM-$C^{Mcm}_{12}\delta_{112}$ and CaM-WT shown as a function of the concentration ratio of CaM:WpOCNC with fits from Equation (S5) (Middle Right and Bottom Left).

Table S5. Percent of Cys Containing Protein Labeled by Mcm-Mal

	CaM-$C^{Mcm}_{12}\delta_{112}$	αS-$C^{Mcm}_{62}\ \delta_{94}$	αS-$C^{Mcm}_{114}\ \delta_{94}$
Percent Labeled	90.1 %	77.3 %	67.2 %

The percent of Cys containing protein labeled by Mcm-Mal was determined from the ratio of the concentrations of Mcm and Acd calculated from UV absorbance spectra (Figs S16 and S21), using the previously described extinction coefficients. These values likely deviate from the true labeling percentage due to background and scattering profiles within the obtained spectra.

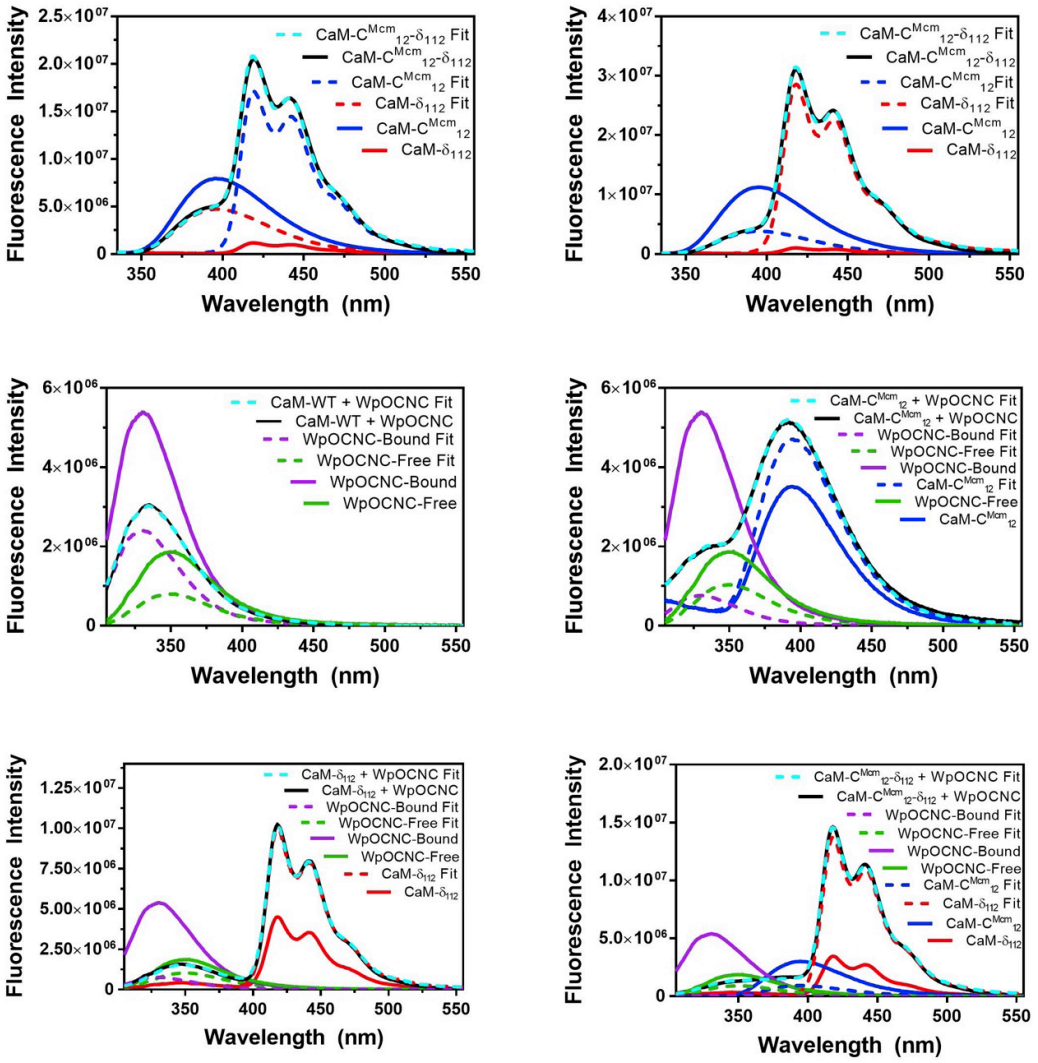

Fig. S18 CaM Steady State FRET Measurements. Plots display the background subtracted (solid) and fit (dashed) spectra for CaM-$C^{Mcm}_{12}\delta_{112}$ (Top Left) following excitation at 325 nm, CaM-$C^{Mcm}_{12}\delta_{112}$ bound to WpOCNC (Top Right) following excitation at 325 nm, WpOCNC bound to wild-type CaM (Middle Left) following excitation at 295 nm, CaM-C^{Mcm}_{12} bound to WpOCNC (Middle Right) following excitation at 295 nm, CaM-δ_{112} bound to WpOCNC (Bottom Left) following excitation at 295 nm and CaM-$C^{Mcm}_{12}\delta_{112}$ bound to WpOCNC (Bottom Right) following excitation at 295 nm. WpOCNC-Free spectra were obtained from measurement of WpOCNC in buffer, while the WpOCNC-Bound spectrum was obtained from measuring WpOCNC bound to wild-type CaM at a 2:1 ratio of protein to peptide with final peptide concentration of 1 μM.

Stopped-Flow Measurements. Stopped-flow experiments were performed with 1 μM Mcm/Acd labelled CaM and 2 μM pOCNC peptide. Each measurement was taken in triplicate following mixing of 20 μL of protein and 20 μL of peptide. For each mixing event the fluorescence emission of Acd (440 ± 40 nm) following excitation of Trp at 295 nm or Mcm at 325 nm. For each measurement, 15000 points were collected over a time range of 30 milliseconds. Nonlinear fits were performed in GraphPad Prism 7.00 where each measurement was fit over the entire time window to the equation

$$Y = Y_0 + Y_M \times \exp(-k \times x) \quad \text{(S6)}$$

In Eq. S6, Y is the fluorescence intensity as a function of time, x, where Y_0 is the maximum intensity and Y_M is the difference between the maximum intesnity and intensity at time zero. The resulting fit values for each curve and the resulting averages are seen in Table S5.

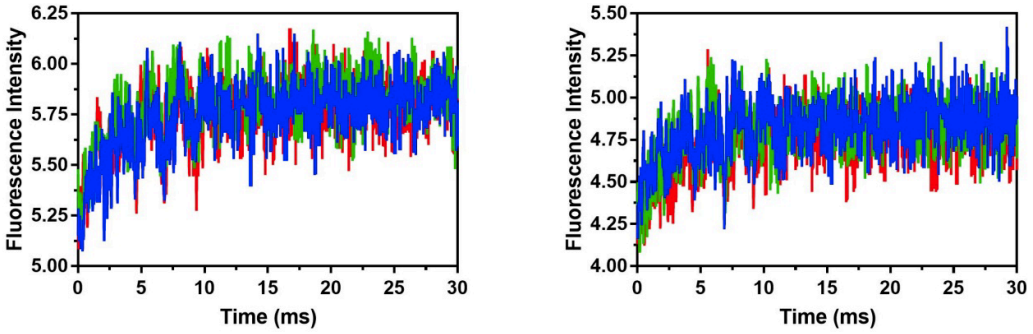

Fig. S19 CaM Stopped-Flow FRET Measurements. Acd emission of CaM-$C^{Mcm}_{12}\delta_{112}$ during binding of WRRIAR was monitored following excitation of Mcm at 325 nm (left) or Trp at 295 nm (right). Acd emission was monitored at 440 ± 40 nm using an Edmund Optics filter. Each plot contains three single stopped-flow shots which were collected following four wasted shots. Protein and peptide were mixed in a 1:2 concentration ratio producing final concentrations of 0.5 μM protein.

Table S6. Stopped-Flow Data Fitting

Parameter	Ex. 295 nm	Std. Dev.	Ex. 325 nm	Std. Dev.
Y_0	4.814	0.028	5.821	0.027
Y_M	-0.517	0.072	-0.531	0.051
k	0.338	0.093	0.306	0.040

Comparison of CaM FRET Data to Other Structural Data. The calculated distances obtained from the experimental Mcm/Acd FRET measurements can be compared to published NMR structures of CaM in the peptide-bound (PDB ID 1SY9) and free (PDB ID 1X02) forms.[7, 8] We selected three representative substructures from the ensembles of 20 low energy structures reported for each PDB entry. Rather than simply calculate the distances between residues 12 and 112 from Cα to Cα, we manually placed into these PDB structures models of the C^{Mcm} chromophore (both *R* and *S* adducts) and Acd chromophore (two sidechain rotamers designated A and B in Fig. S17) generated from AM1 minimized structures in Gaussian 09.[9] For Acd, the sidechain orientation was determined by making a Phe mutation at positon 112 in PyMol and aligning the Acd chromophore with the Phe sidechain. For C^{Mcm}, a Cys mutant was made at position 12 in PyMol and the sulfur atom in the Mcm model was aligned with the Cys sulfur. The Mcm chomophore was then rotated about the Cα-Cβ-S-Cmaleimide bond to minimize steric clashes. The Mcm and Acd models used are shown in Figure S17. The distances between the highlighted (black arrows) atoms were determined and averaged to identify the center-to-center distance between the two chromophores. The values from the two Acd rotamers and the *R* and *S* adducts of the Mcm chromophore are reported in Table S6. Ranges for these values were reported in the main text.

Table S7. CaM Structural Model Data

PDB ID	Distance (Å)	PDB ID	Distance (Å)	PDB ID	Distance (Å)
1X02 – 14AS	30.5	1X02 – 3AS	36.7	1X02 – 7AS	37.3
1X02 – 14BS	28.8	1X02 – 3BS	33.8	1X02 – 7BS	34.9
1X02 – 14AR	25.3	1X02 – 3AR	36.6	1X02 – 7AR	42.3
1X02 – 14BR	23.1	1X02 – 3BR	33.6	1X02 – 7BR	40.7
	26.9 ± 3.4		35.2 ± 1.7		38.8 ± 3.3
1SY9 – 11AS	16.5	1SY9 – 3AS	21.9	1SY9 – 17AS	20.2
1SY9 – 11BS	15.5	1SY9 – 3BS	15.2	1SY9 – 17BS	18.1
1SY9 – 11AR	16.2	1SY9 – 3AR	21.7	1SY9 – 17AR	20.0
1SY9 – 11BR	15.8	1SY9 – 3BR	19.8	1SY9 – 17BR	18.3
	16.0 ± 0.4		19.1 ± 1.1		19.6 ± 3.1

Structure names correspond to PDB ID, followed by substructure number, Acd A or B rotamer, and C^{Mcm} *R* or *S* stereochemistry at starred carbon in Figure S17.

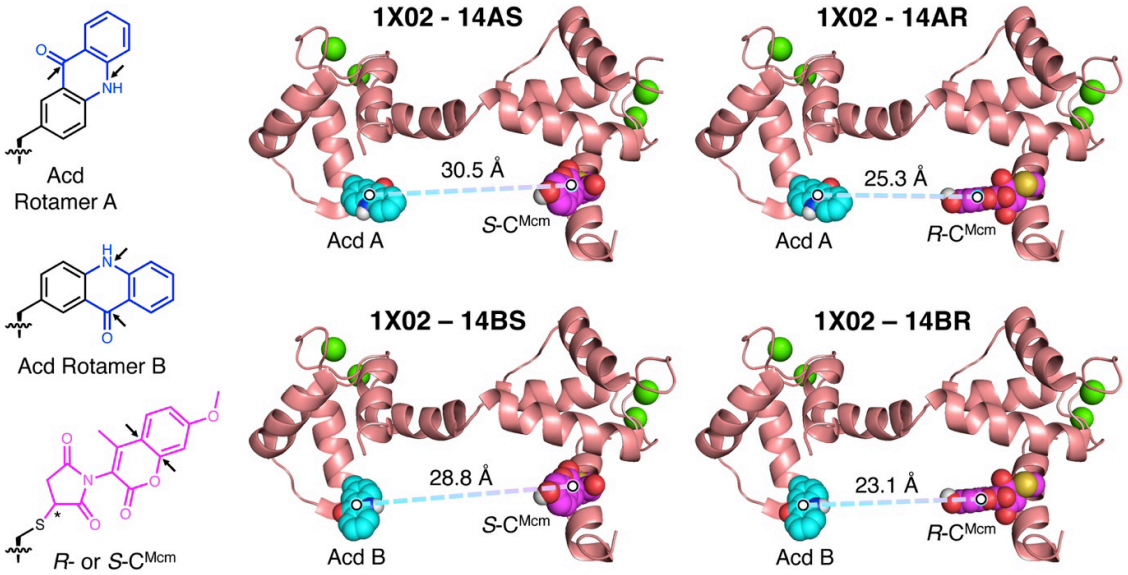

Fig. S20 CaM Structural Models. Left: Chromophore structures used in modelling Acd or C^{Mcm} in CaM structures. Acd rotamers were superimposed on the lowest energy rotamer of a Phe_{112} mutant in each CaM structure. *R*- or *S*-Mcm-Mal thiol adducts were docked onto Cys_{12} mutants in each CaM structure. The distances between the atoms indicated by arrows were computed and averaged to determine the chromophore separation for comparison to FRET data. Right: Example of the four models of Mcm/Acd-labelled CaM generated from PDB-ID 1X02 structure 14, corresponding to Acd rotamer A or B with *R*- or *S*-C^{Mcm}. Other structures used in the analysis reported in Table S6 were generated in a similar fashion from structures in PDB ID 1X02 or 1SY9.

αS FRET Measurements

αS Fluorescence Measurements. Purified C^{Mcm}-labelled, δ-labelled, and C^{Mcm}/δ double-labelled αS proteins were dialyzed into αS buffer. Protein concentrations were determined by absorption spectroscopy (C^{Mcm}: ε_{325} = 19,010 $M^{-1}cm^{-1}$ Acd: ε_{386} = 5,700 $M^{-1}cm^{-1}$).[6, 10] Background corrections were performed using ale 1.2.[11] Fluorescence steady-state spectra were obtained at protein concentrations of ~0.5 μM while fluorescence lifetimes were acquired at ~2 μM. Buffers containing varying concentrations of trimethylamine *N*-oxide (TMAO) in 20 mM Tris and 100 mM NaCl were prepared on the day of the spectroscopy experiments, and the pH of each buffer was readjusted to 7.5 following the addition of TMAO. Both steady-state and lifetime measurements were performed at concentrations of 0, 2, and 4 M TMAO. Steady-state measurements were performed with direct excitation of Mcm at 325 nm, measuring emission from 335-600 nm, with all slit widths set to 5 nm, a step size of 1 nm, and an integration time of 0.25 s per step. Direct excitation of Acd was performed at 386 nm, measuring from 396-600 nm with the same slit width, step size, and integration time.

Steady State Fluorescence Data Fitting and FRET Calculation. Due to the significant overlap of the Mcm and Acd emission spectra, deconvolution was required to determine the relative Mcm quenching due to FRET. Fitting of spectra containing Mcm and Acd double-labelled protein was performed by minimizing the square difference between the spectra from the double-labelled protein and a sum of linearly weighted single-labelled spectra using the following equation

$$\sum_{\lambda}\left(I(\lambda)_{DA} - \left(AI(\lambda)_{D} - BI(\lambda)_{A}\right)\right)^2 \rightarrow \min \qquad \text{(S7)}$$

Here, $I(\lambda)_{DA}$, $I(\lambda)_{D}$ and $I(\lambda)_{A}$ represent the fluorescence intensity at a given wavelength from protein which was double-labelled, single-labelled with only the FRET donor, and single-labelled with only the FRET acceptor, respectively. *A* and *B* are linear weights of the

donor and acceptor spectra and are wavelength invariant. The Solver function in Microsoft Excel was used to vary the values of *A* and *B* to minimize the sum of this square difference across all emission wavelengths. The FRET efficiency (E_{FRET}) was then directly obtained from the linear weight of donor spectrum, *A*, where $A = 1\text{-}E_{FRET}$.

For CaM experiments, distances were determined using the canonical Förster equation (Eq. S4). Error bars for CaM experiments were obtained via propagation of error through the determination of *A* and the canonical Förster equation. Interfluorophore distance values for αS experiments were calculated using a polymer scaled version of the Förster equation of the form

$$E_{FRET} = \sum_r P(r) / \left(1 + (r/R_0)^6\right) \tag{S8}$$

were the probability distribution was set to the functional form for a Gaussian chain.

$$P(r) = 4\pi r^2 \left(\frac{3}{2\pi\langle r^2\rangle}\right)^{3/2} \exp\left(-\frac{3}{2}\frac{r^2}{\langle r^2\rangle}\right) \tag{S9}$$

Error bars were obtained via propagation of experimental error through both determination of *A* and distance determination using the Gaussian-chain scaled Förster equation.

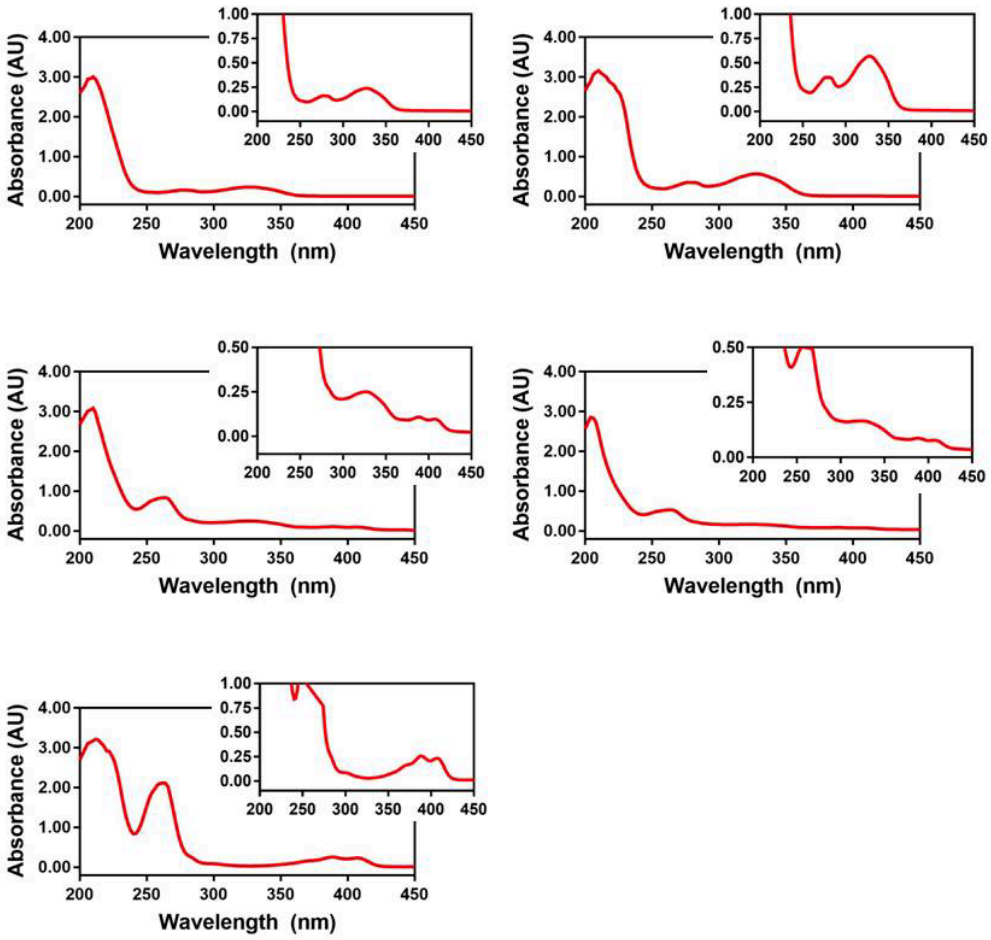

Fig. S21 αS Absorbance Measurements. Absorbance spectra of αS-C$^{Mcm}_{62}$ (Top Left), αS-C$^{Mcm}_{114}$ (Top Right) αS-C$^{Mcm}_{62}$ δ$_{94}$ (Middle Left), αS-C$^{Mcm}_{114}$ δ$_{94}$ (Middle Right) and αS-δ$_{94}$ (Bottom Left).

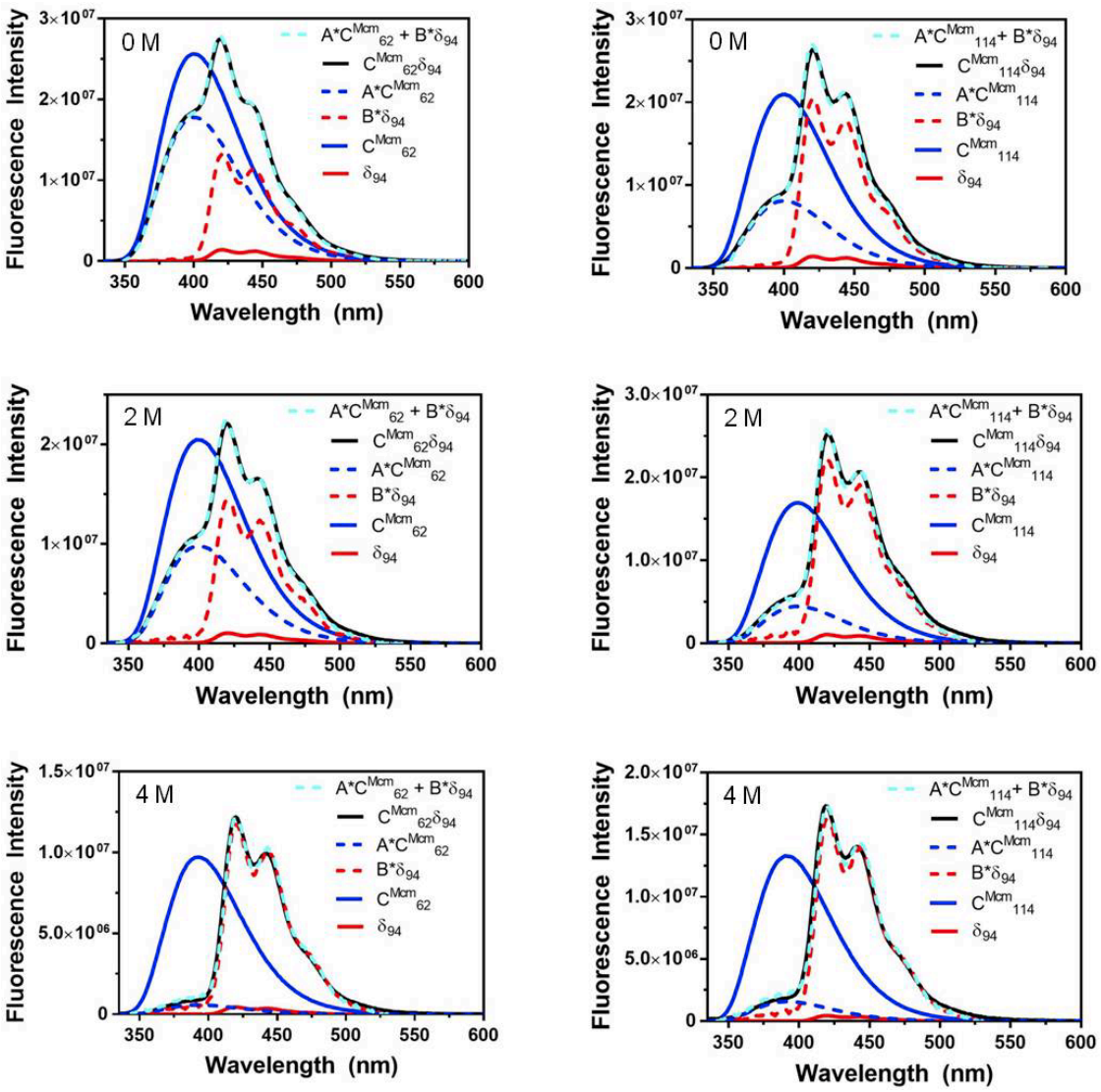

Fig. S22 αS Fluorescence Spectra and FRET Fitting Results. Donor-only (C^{Mcm}, solid blue line), acceptor-only (δ, solid red line), or double-labelled (C^{Mcm}/δ, solid black line) spectra are shown overlayed with the results of fitting the double-labelled spectra to a weighted sum of the single-labelled spectra (light blue dashed line). The weighted component spectra are shown in dashed blue (donor-only) and dashed red (acceptor-only) lines. Spectra were acquired in buffer containing 0, 2, or 4 M TMAO with excitation at 325 nm.

Fluorescence Lifetime Data Fitting and FRET Calculation. Fluorescence lifetime measurements were acquired via time-correlated single photon counting using a 340 nm LED light source. Lifetime spectra were all acquired at 380 nm with slit widths ≤ 8 nm and collection over a 199 ns time window, which was divided into 4096 lifetime bins. Collection was terminated when a single bin reached a count of 10,000 photons. TCSPC data were fit to single or bi-exponential decays using PowerFit-10. The FRET efficiency (E_{FRET}) was calculated as one minus the ratio of the Mcm lifetime in the presence of Acd to the Mcm lifetime in the absence of Acd.

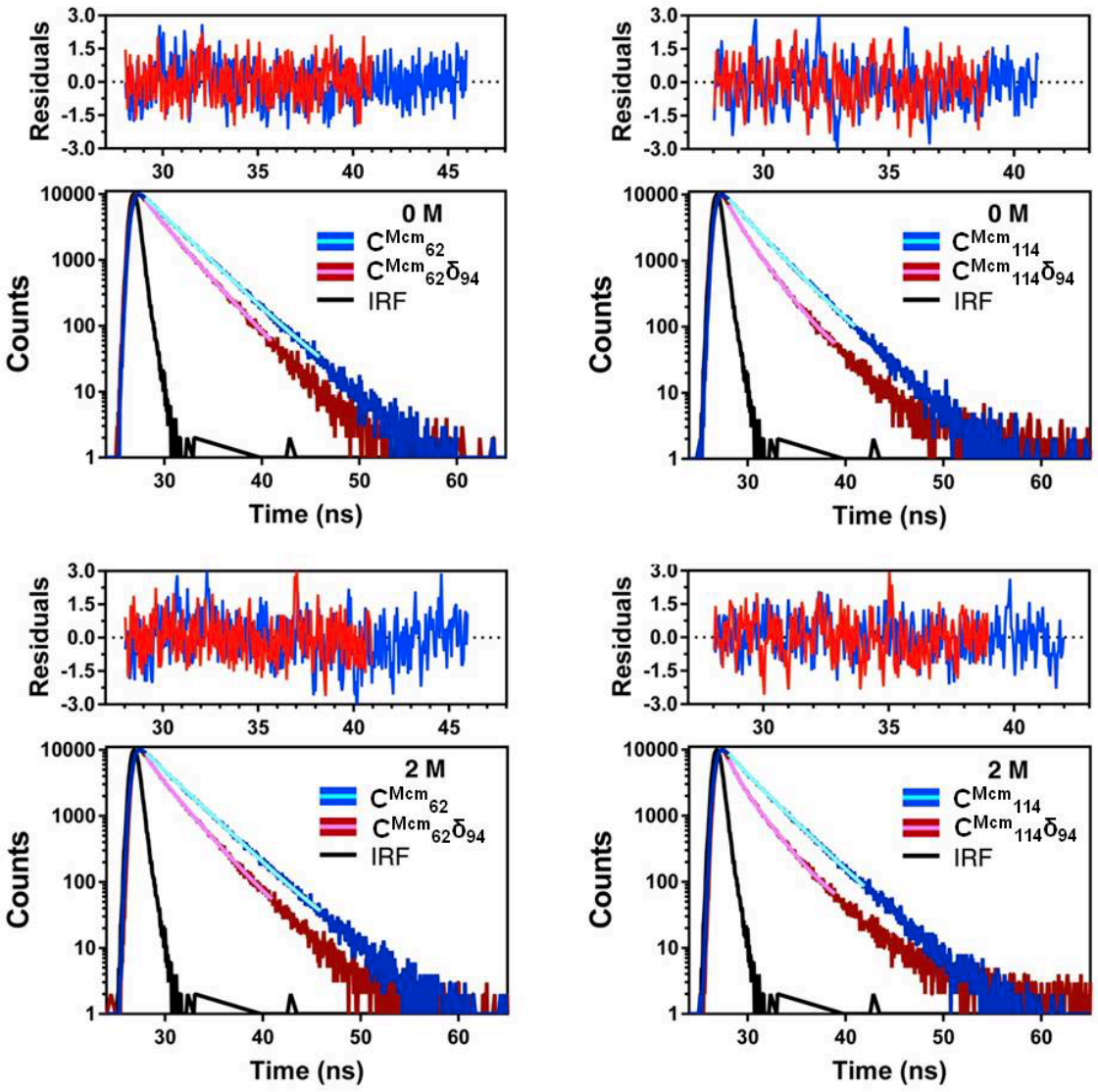

Fig. S23a αS Fluorescence Spectra and FRET Fitting Results. TCSPC data sets in 0 M or 2 M TMAO are shown for donor-only (C^{Mcm}, dark blue line) or double labelled (C^{Mcm}/δ, dark red line). Bi-exponential fits to the data are shown in light blue (donor only) or pink (double labelled); the instrument response function (IRF) is shown in black. Weighted residuals are shown in corresponding colors above each fluorescence lifetime plot.

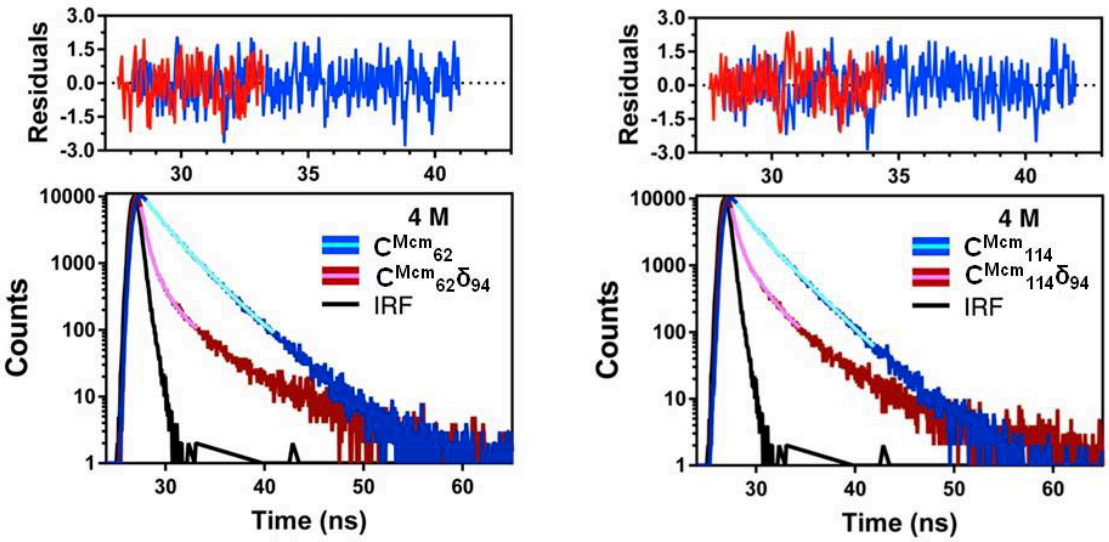

Fig. S23b αS Fluorescence Spectra and FRET Fitting Results. TCSPC data sets in 4 M TMAO are shown for donor-only (C^{Mcm}, dark blue line) or double labelled (C^{Mcm}/δ, dark red line). Bi-exponential fits to the data are shown in light blue (donor only) or pink (double labelled); the instrument response function (IRF) is shown in black. Weighted residuals are shown in corresponding colors above each fluorescence lifetime plot.

Table S8. TCSPC Fluorescence Lifetime Values

Proteim	TMAO	τ_1	τ_2	Amplitude$_1$	Amplitude$_2$	$\tau_{Avg.}$	χ^2	E_{FRET}
αS-C$^{Mcm}_{62}$	0 M	3.10	-	2.47	-	3.10	0.90	-
	2 M	3.12	-	3.03	-	3.12	1.16	-
	4 M	2.80	0.86	0.79	0.55	2.01	0.93	-
αS-C$^{Mcm}_{114}$	0 M	2.85	0.95	1.01	0.25	2.47	1.20	-
	2 M	3.03	0.96	1.00	0.32	2.53	0.83	-
	4 M	3.01	1.13	0.68	0.76	2.12	0.96	-
αS-C$^{Mcm}_{62}$δ$_{94}$	0 M	2.74	1.29	0.93	0.50	2.23	0.84	0.28
	2 M	2.60	1.01	1.02	0.78	1.92	0.95	0.39
	4 M	1.90	0.39	0.17	2.81	0.48	0.97	0.76
αS-δ$_{94}$C$^{Mcm}_{114}$	0 M	2.17	0.71	0.70	0.71	1.43	1.07	0.42
	2 M	0.82	2.31	0.67	1.10	1.38	1.04	0.45
	4 M	2.07	0.42	0.28	2.68	0.57	0.99	0.73

Comparison of αS FRET Data to Other Structural Data. The calculated distances obtained from the experimental Mcm/Acd FRET measurements were compared to published structural ensembles. The two ensembles were previously published in Allison *et al*. and Nath *et al*., derived from a molecular dynamics simulation restrained with paramagetic relaxation enhancement data and a Monte Carlo simulation with constraints from FRET, respectively.[12-14] To obtain distances for comparisons, the distances between Cα atoms for every residue pair in the sequence were extracted from each structure within each ensemble. Since αS is intrinsically disordered, it is unlikely that the structural ensembles represent the full distribution of states, therefore distances were averaged in a Flory-scaling like protocol similar to the analysis in Nath *et al*.[12] For each ensemble, the inter-residue distances were averaged over all residue pairs spaced by the same primary sequence separation over all structures, rather than just averaging over a single specific residue pair over all structures. The average and standard deviation of the inter-residue distance as a function of primary sequence separation is shown in Figure S20, along with the probe separation distance calculated from the experimental Mcm-Acd FRET efficiency via the gaussian chain polymer-scaled version of the Förster equation. Since there are no published ensembles for the structure of αS in the presence of TMAO, this comparison could only be performed for measurements in the absence of TMAO.

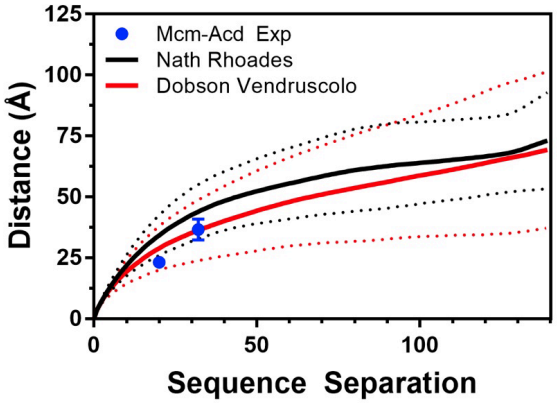

Fig. S24 Mcm/Acd FRET Data Compared to Previous Structural Models of αS Ensembles.

References

1. N. Myung, S. Connelly, B. Kim, S. J. Park, I. A. Wilson, J. W. Kelly and S. Choi, *Chem. Commun.*, 2013, **49**, 9188-9190.

2. S. Batjargal, C. R. Walters and E. J. Petersson, *J. Am. Chem. Soc.*, 2015, **137**, 1734-1737.

3. I. Sungwienwong, Z. M. Hostetler, R. J. Blizzard, J. J. Porter, C. M. Driggers, L. Z. Mbengi, J. A. Villegas, L. C. Speight, J. G. Saven, J. J. Perona, R. M. Kohli, R. A. Mehl and E. J. Petersson, *Org. Biomol. Chem.*, 2017, **15**, 3603-3610.

4. C. M. Haney, C. L. Cleveland, R. F. Wissner, L. Owei, J. Robustelli, M. J. Daniels, M. Canyurt, P. Rodriguez, H. Ischiropoulos, T. Baumgart and E. J. Petersson, *Biochemistry*, 2017, **56**, 683-691.

5. C. M. Haney, R. F. Wissner, J. B. Warner, Y. X. J. Wang, J. J. Ferrie, D. J. Covell, R. J. Karpowicz, V. M. Y. Lee and E. J. Petersson, *Org. Biomol. Chem.*, 2016, **14**, 1584-1592.

6. L. C. Speight, A. K. Muthusamy, J. M. Goldberg, J. B. Warner, R. F. Wissner, T. S. Willi, B. F. Woodman, R. A. Mehl and E. J. Petersson, *J. Am. Chem. Soc.*, 2013, **135**, 18806-18814.

7. G. M. Contessa, M. Orsale, S. Melino, V. Torre, M. Paci, A. Desideri and D. O. Cicero, *J. Biomol. NMR*, 2005, **31**, 185-199.

8. M. Kainosho, T. Torizawa, Y. Iwashita, T. Terauchi, A. Mei Ono and P. Güntert, *Nature*, 2006, **440**, 52-57.

9. M. J. Frisch, G. W. Trucks, H. B. Schlegel, G. E. Scuseria, M. A. Robb, J. R. Cheeseman, J. Montgomery, J. A., T. Vreven, K. N. Kudin, J. C. Burant, J. M. Millam, S. S. Iyengar, J. Tomasi, V. Barone, B. Mennucci, M. Cossi, G. Scalmani, N. Rega, G. A. Petersson, H. Nakatsuji, M. Hada, M. Ehara, K. Toyota, R. Fukuda, J. Hasegawa, M. Ishida, T. Nakajima, Y. Honda, O. Kitao, H. Nakai, M. Klene, X. Li, J. E. Knox, H. P. Hratchian, J. B. Cross, V. Bakken, C. Adamo, J. Jaramillo, R. Gomperts, R. E. Stratmann, O. Yazyev, A. J. Austin, R. Cammi, C. Pomelli, J. W. Ochterski, P. Y. Ayala, K. Morokuma, G. A. Voth, P. Salvador, J. J. Dannenberg, V. G. Zakrzewski, S. Dapprich, A. D. Daniels, M. C. Strain, O. Farkas, D. K. Malick, A. D. Rabuck, K. Raghavachari, J. B. Foresman, J. V. Ortiz, Q. Cui, A. G. Baboul, S. Clifford, J. Cioslowski, B. B. Stefanov, G. Liu, A. Liashenko, P. Piskorz, I. Komaromi, R. L. Martin, D. J. Fox, T. Keith, M. A. Al-Laham, C. Y. Peng, A. Nanayakkara, M. Challacombe, P. M. W. Gill, B. Johnson, W. Chen, M. W. Wong, C. Gonzalez and J. A. Pople, *Gaussian 09*, Gaussian, Inc., 2009

10. A. Szymanska, K. Wegner and L. Lankiewicz, *Helv. Chim. Acta*, 2003, **86**, 3326-3331.

11. ale, UV-Vis-IR Spectral Software 1.2 FluorTools, http://www.fluortools.com/).

12. A. Nath, M. Sammalkorpi, David C. DeWitt, Adam J. Trexler, S. Elbaum-Garfinkle, Corey S. O'Hern and E. Rhoades, *Biophys. J.*, 2012, **103**, 1940-1949.

13. M. Varadi, S. Kosol, P. Lebrun, E. Valentini, M. Blackledge, A. K. Dunker, I. C. Felli, J. D. Forman-Kay, R. W. Kriwacki, R. Pierattelli, J. Sussman, D. I. Svergun, V. N. Uversky, M. Vendruscolo, D. Wishart, P. E. Wright and P. Tompa, *Nucleic Acids Res.*, 2014, **42**, D326-D335.

14. J. R. Allison, P. Varnai, C. M. Dobson and M. Vendruscolo, *J. Am. Chem. Soc.*, 2009, **131**, 18314-18326.